

# TRS: Transferability Reduced Ensemble via Encouraging Gradient Diversity and Model Smoothness

Zhuolin Yang<sup>1</sup> \* Linyi Li<sup>1</sup> \* Xiaojun Xu<sup>1\*</sup> Shiliang Zuo<sup>1</sup>  
 Qian Chen<sup>2</sup> Benjamin Rubinstein<sup>3</sup> Ce Zhang<sup>4</sup> Bo Li<sup>1</sup>

<sup>1</sup> University of Illinois at Urbana-Champaign, USA {xiaojun3, linyi2, zhuolin5, szuo3, lbo}@illinois.edu

<sup>2</sup> Tencent Inc., China qianchen@tencent.com

<sup>3</sup> University of Melbourne, Australia benjamin.rubinstein@unimelb.edu.au

<sup>4</sup> ETH Zurich, Switzerland ce.zhang@inf.ethz.ch

## Abstract

*Adversarial Transferability* is an intriguing property of adversarial examples – a perturbation that is crafted against one model is also effective against another model, which may arise from a different model family or training process. To better protect ML systems against such adversarial attacks, several questions are raised: what are the sufficient conditions for adversarial transferability? Is it possible to bound such transferability? Is there a way to reduce the transferability in order to improve the robustness of an ensemble ML model? To answer these questions, in this work we aim to first theoretically analyze and outline checkable sufficient conditions for transferability between models; then propose a practical algorithm to reduce transferability between base models within an ensemble to improve its robustness. Our theoretical analysis, as the first work, shows that only the orthogonality between gradients of different models is not enough to ensure low adversarial transferability; in the meantime, the model smoothness is an important factor to impact the transferability together with gradient orthogonality. In particular, we provide a lower bound of adversarial transferability based on model gradient similarity, as well as an upper bound for low risk classifiers based on gradient orthogonality and model smoothness. We demonstrate that under the condition of gradient orthogonality, smoother classifiers will guarantee lower adversarial transferability. Finally, inspired by our theoretical analysis, we propose an effective Transferability Reduced Smooth-ensemble (TRS) training strategy to train a robust ensemble with low transferability by enforcing model smoothness and gradient orthogonality between base models. We conduct extensive experiments on TRS and compare with 6 state-of-the-art ensemble baselines against 8 whitebox attacks on different datasets, showing that the proposed TRS outperforms all baselines significantly. We believe our analysis on adversarial transferability will not only provide further understanding on predictions of ML models, but also inspire future research towards developing robust ML models taking these adversarial transferability properties into account.

## 1 Introduction

Machine learning systems, especially those based on deep neural networks (DNNs), have been widely applied in numerous settings, including image recognition [30], speech recognition [21], natural language processing [51], and malware detection [11]. However, recently it has shown that DNNs are vulnerable to adversarial examples, which are able to mislead DNNs by adding small magnitude of perturbations to the original instances [52; 20]. There have also been a number of efforts exploring adversarial examples in general machine learning systems beyond those on DNNs [2; 3; 33; 34; 18]. Several attack strategies have

---

\*The authors contribute equally.

been proposed so far to generate such adversarial examples in both digital and physical environments [40; 36; 55; 56; 17; 31]. For instance, several work has shown that such adversarial examples are effective in the physical world [31; 17]. It is thus clear that such adversarial attacks are a common risk across different learning systems and may exist in different domains.

Intriguingly, though most of the attack strategies mentioned above require access to the information of target machine learning models (whitebox attacks), it has been found that even without knowledge about the exact target model, adversarial examples generated against another model can *transferably* attack the target victim model, giving rise to blackbox attacks [43; 44]. This property of adversarial transferability poses great threat to the real-world DNN-based systems since the attacker could succeed even without intrusion to the target ML system. Some work have been conducted to understand adversarial transferability [54; 37; 14]. However, a rigorous theoretical analysis or explanation for transferability is still lacking in the literature. In addition, although developing robust ensemble models to limit transferability shows great potential towards practical robust learning systems, only *empirical* observations have been made in this line of research [42; 25; 57]. *Can we deepen our theoretical understanding on transforability? Can we then take advantage of any new theoretical understanding to reduce the transferability and therefore generate better robust ensemble models?*

In this paper, we focus on these two questions. From the theoretical side, we are interested in the sufficient conditions under which the transferability can be *lower bounded* or *upper bounded*, both of which could lead to insights that could have profound empirical implications: *An upper bound on transferability could potentially deliver a new optimization objective when training robust ensemble models, while a lower bound on transferability could help avoid “doomed” scenarios.*

Our theoretical arguments provides the *first* theoretical interpretation for the sufficient conditions of transferability. Intuitively, as illustrated in Figure 1, we show that the commonly used gradient orthogonality (low cosine similarity) between learning models cannot directly imply low transferability; on the other hand, orthogonal and smoothed models would limit transferability. Our analysis is inspired by this intuition, with a focus on understanding the impact of *model smoothness* and *gradient cosine similarity* on transferability. In particular, the existing work on understanding the adversarial transferability focuses on the empirical evaluation, which mainly rely on minimizing the gradient cosine similarity; while other factors such as model smoothness are not outlined or studied. For instance, Pang et al. [42] propose to diversify the models’ output confidence and empirically shows that it limits the transferability to some extent. Yang et al. [57] propose to diversify the distilled features learned from the models by penalizing feature overlaps during training. However, there is no explanation on how the models evolve to be diversified quantitatively. A large-scale empirical study [14] summarizes three main factors that affect the transferability: the magnitude of input gradients, the gradient similarity, and the variability of the loss landscape, while the theoretical justifications of these factors are still open. In this paper, we prove that the model smoothness and gradient similarity are the key factors that contributes to the transferability both theoretically, and smooth models with orthogonal gradients can guarantee low transferability. We also verify our theoretical analysis based on extensive experiments. Interestingly, from another point of view, we identify that the model smoothness we analyzed here is actually the precise key factor covered by the broad definition based on the large-scale empirical studies in [14]: the variability for the loss landscape or the so-called “complexity” of the model,

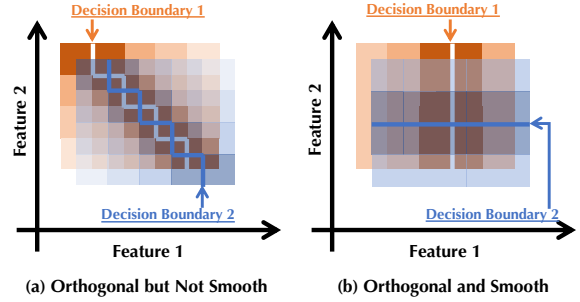


Figure 1: An illustration of the relationship between *transferability*, *gradient orthogonality*, and *smoothness*. (a) Gradient orthogonality alone cannot guarantee transferability as the decision boundaries between two classifiers can be arbitrarily close yet have orthogonal gradients almost everywhere; (b) Gradient orthogonality with smoothness provides a stronger guarantee on diversity, as our theorems will show.

since well-trained smoother models have smaller variance in its loss landscape and smaller model complexity.

In addition, based on the Taylor expansion and Markov’s inequality, we derive a lower bound on transferability between two low risk classifiers based on model smoothness and loss gradient similarity for the  $\ell_2$  norm bounded adversarial examples. Beyond such common attack types, we also derive a lower bound for transferability from the perspective of data distribution distance, *i.e.* under the condition that the distance between the benign and adversarial distributions is bounded. Both lower bounds illuminate mechanisms of transferability under different scenarios. Besides, we also prove an upper bound on transferability, demonstrating that transferability can be upper bounded by model smoothness, model risks, and the similarity of their loss gradients.

Under an empirical lens, inspired by our theoretical results, we propose a simple yet effective approach, **Transferability Reduced Smooth-ensemble** (TRS) to limit transferability between base models within an ensemble and therefore improve its robustness. In particular, we enforce the smoothness of models as well as reduce the loss gradient similarity between models to introduce global model orthogonality.

We conduct extensive experiments to evaluate TRS in terms of the robustness of the ensemble against the strong white-box attacks, as well as its ability to limit transferability across the base models. We compare the proposed TRS with existing state-of-the-art baseline ensemble approaches in the literature including ADP [42], GAL [25], DVERGE [57], etc. We apply multiple strong whitebox attacks such as PGD [38], FGSM [20], C&W [7], and EAD [10] to simulate a powerful adversary and provide an empirically tighter upper bound of the ML robustness against strong adversarial attacks. On both MNIST and CIFAR10 datasets, when compared with the baselines, we show that (1) TRS requires smaller or comparable training time; and (2) TRS achieves the state-of-the-art ensemble robustness, outperforming others by a large margin. (3) TRS effectively reduces the transferability among base models within an ensemble which indicates its robustness against whitebox and blackbox attacks. (4) Both loss terms in TRS induce robustness for an ensemble by constraining different sufficient conditions of transferability.

**Contributions.** In this paper, we make the first attempt towards theoretical understanding of adversarial transferability, and providing practical approaches to developing robust ML ensembles. Our contributions are summarized as below.

- (1) We provide a general theoretical analysis framework for adversarial transferability. We prove the lower bounds on transferability between low risk classifiers for both  $\ell_p$  norm bounded and distribution enabled adversarial examples.
- (2) We prove an upper bound of transferability based on model similarity and smoothness, emphasizing the importance of model smoothness in decreasing the transferability between models, which is aligned with the conclusions of existing large-scale empirical studies. We show that with smoother models, both the lower and upper bounds of transferability are tighter.
- (3) We propose a simple yet effective approach TRS to train a robust ensemble by enforcing model smoothness and reducing loss gradient similarity between models.
- (4) We conduct extensive experiments to evaluate the robustness of the proposed ensemble model, and show that it outperforms the state-of-the-art robust ensemble approaches on different datasets against a range of attacks.

## 2 Related Work

**Adversarial vulnerabilities of deep neural networks.** Since the early studies on adversarial examples against deep neural networks [52], the adversarial vulnerabilities of deep neural networks has raised great concerns these years, especially for security-critical scenarios, such as autonomous driving and drug

design [31; 17; 50]. There has been a series of work on adversarial evasion attacks, including both whitebox and blackbox attacks [20; 8; 1; 55]. Corresponding defenses have also been extensively studied, including both empirical defenses [38; 47] which are usually been adaptive attacked again [1; 53], and provable robust ML defenses [27; 12; 35]). Besides, the explanation of such vulnerabilities have also provided further understanding on the potential reasons and ways towards improving ML robustness [54; 37; 14].

**Adversarial transferability.** The adversarial transferability between different ML models is an intriguing avenue of studies. Papernot et al. [46] explored the limitation of adversarial examples and showed that, while some instances are more difficult to manipulate than the others, these adversarial examples usually transfer from one model to another. It has also been found that the transferability property holds across different classification models, such as support vector machines, decision trees, and neural networks. This property exists not only across classifiers with the same underlying model, but also in the cross-model cases [43]. Demontis et al. [14] later analyzed transferability for both evasion and poisoning attacks. Tramèr et al. [54] empirically investigated the subspace of adversarial examples that enables transferability between different models: though their results provide a non-zero probability guarantee on the transferability, they did not quantify the probability with which the adversarial examples transfer.

**Transferability based attacks and diversified robust ensemble as defenses.** Given that the adversarial transferability implies the vulnerability of machine learning models even without being accessed by attackers, different blackbox attacks have been proposed in practice, such as for applications where the classifier is deployed in the cloud [44]. To defend against these transferability based attacks, Pang et al. [42] proposed a class entropy based adaptive diversity promoting approach to enhance the ML ensemble robustness. Recently, Yang et al. [57] proposed DVERGE, a robust ensemble training approach that diversifies the non-robust features of base models via an adversarial training enabled objective function. However, these approaches do not provide theoretical justification for adversarial transferability, and there is still room to improve the ML ensemble robustness based on in-depth understanding on the sufficient conditions of transferability. In this paper, we aim to provide both theoretical understanding of transferability and the lower and upper bounds for it, and empirically compare the proposed robust ML ensemble inspired by our theoretical analysis with existing approaches to push for a tighter empirical upper bound for the ensemble robustness.

### 3 Preliminaries and Method Overview

In this section, we first discuss the general threat model, and then provide an overview of our proposed TRS method and its theoretical motivation. Our theoretical analysis in Section 4 will follow the same threat model defined here.

#### 3.1 Threat Model

**Preliminaries.** We consider neural networks for classification tasks. Let  $\mathcal{X}$  be the *input space* of the model (e.g. the set of all possible images for an image classification task). Let  $\mathcal{Y}$  denote the set of classes (i.e., labels) the models would output. If there are  $C$  classes,  $\mathcal{Y} = \{1, 2, \dots, C\}$ . The neural network is modeled as a mapping function  $\mathcal{F}$  (or  $\mathcal{G}$ ) from  $\mathcal{X}$  to  $\mathcal{Y}$ . We will study the transferability between two models  $\mathcal{F}$  and  $\mathcal{G}$  hereinafter. For notation simplicity, in later definitions we will only use the derived notations for  $\mathcal{F}$ , which are similar  $\mathcal{G}$ .

For a given input  $x \in \mathcal{X}$ , the classification model  $\mathcal{F}$  first predicts the confidence score for each label  $y \in \mathcal{Y}$ , denoted as  $f_y(x)$ . These confidence scores across different labels sum up to 1, i.e.,  $\sum_{y \in \mathcal{Y}} f_y(x) = 1, \forall x \in \mathcal{X}$ . The model  $\mathcal{F}$  will output the label with highest confidence score as the prediction:  $\mathcal{F}(x) = \arg \max_{y \in \mathcal{Y}} f_y(x)$ .

For model  $\mathcal{F}$ , there is usually a model-dependent loss function  $\ell_{\mathcal{F}} : \mathcal{X} \times \mathcal{Y} \mapsto \mathbb{R}_+$ , which is the composition

of a standard training loss (e.g., cross-entropy loss)  $\ell$  and the model's confidence score  $f(\cdot)$ : for  $(x, y) \in (\mathcal{X}, \mathcal{Y})$ ,  $\ell_{\mathcal{F}}(x, y) := \ell(f(x), y)$ . For instance, when  $\ell$  is the cross-entropy loss,  $\ell_{\mathcal{F}}(x, y) = -\log f_y(x)$ . We further assume that  $\mathcal{F}(x) = \arg \min_{y \in \mathcal{Y}} \ell_{\mathcal{F}}(x, y)$ , i.e., the model's predicted label is the one with minimum loss. This holds for common standard training loss. Neural network models are usually differentiable, i.e., for any  $(x, y) \in (\mathcal{X}, \mathcal{Y})$ ,  $\nabla_x f_y(x)$  exists, and so as  $\nabla_x \ell(f(x), y)$ .

Following the convention, we assume that the *benign* data  $(x, y)$  follows an unknown distribution  $\mathcal{D}$  supported on  $(\mathcal{X}, \mathcal{Y})$ . Under this distribution  $\mathcal{D}$ , we use  $\mathcal{P}_{\mathcal{X}}$  to represent the marginal distribution on  $\mathcal{X}$ . The  $\Pr(E)$  and  $\mathbb{E}[v]$  represent the probability of an event  $E$  and the expected value of a random variable  $v$  under distribution  $\mathcal{D}$ , respectively.

In this paper, by default we will focus on models that are well-trained on the benign dataset, and such models are the most commonly encountered in practice, so their robustness is paramount. This means we will focus on the *low risk* classifiers, which we will formally define in Section 4.1.

Throughout the paper, we focus on the data evasion attacks, where the attacker tries to craft an adversarial example that fools the model to make wrong predictions. It is worth mentioning that through optimizing framework in [14] it is also possible to extend our analysis to data poisoning attacks where the attacker maliciously manipulates the training data to cause model failures, and we leave this as interesting future directions.

*How should we define an adversarial attack?* We first adopt a natural approach to define an attack strategy — the attacker adds an  $\ell_p$  norm bounded perturbation to data instance  $x \in \mathcal{X}$ . In practice, there are two types of attacks, *untargeted attacks* and *targeted attacks*. As previous work observed, the adversarial transferability is different under different attacks [37], and we consider both in our analysis.

**Definition 1** (Adversarial Evasion Attack). *Consider an input  $x \in \mathcal{X}$  with ground truth label  $y \in \mathcal{Y}$ ,  $\mathcal{F}(x) = y$ .*

- *An untargeted attack crafts  $\mathcal{A}_U(x) = x + \delta$  to maximize  $\ell_{\mathcal{F}}(x + \delta, y)$  where  $\|\delta\|_p \leq \epsilon$ .*
- *A targeted attack with adversarial target  $y_t \in \mathcal{Y}$  crafts  $\mathcal{A}_T(x) = x + \delta$  to minimize  $\ell_{\mathcal{F}}(x + \delta, y_t)$  where  $\|\delta\|_p \leq \epsilon$ .*

In this definition,  $\|\delta\|_p$  represents the  $\ell_p$  norm of  $\delta$ , and  $\epsilon$  is a pre-defined *attack radius* that limits the power of the attacker. We may refer to  $\{\delta : \|\delta\|_p \leq \epsilon\}$  as the perturbation ball. The goal of the untargeted attack is to maximize the loss function of the target model against its true label  $y$ . The goal of the targeted attack is to minimize the loss function towards its adversarial target label  $y_t$ .

*How do we formally define that an attack is effective?* We define the attack effectiveness for both targeted and untargeted attacks based on the statistical probability of successful attacks.

**Definition 2**  $((\alpha, \mathcal{F})$ -effective attack). *Consider a input  $x \in \mathcal{X}$  with true label  $y \in \mathcal{Y}$ . An attack is  $(\alpha, \mathcal{F})$ -effective in both untargeted and targeted (with class target  $y_t$ ) scenarios if:*

- *Untargeted:  $\Pr(\mathcal{F}(\mathcal{A}_U(x)) \neq y) \geq 1 - \alpha$ .*
- *Targeted:  $\Pr(\mathcal{F}(\mathcal{A}_T(x)) = y_t) \geq 1 - \alpha$ .*

This definition captures the requirement that an adversarial instance generated by an effective attack strategy is able to mislead the target classification model (e.g.  $\mathcal{F}$ ) based on certain probability  $\alpha$ . The smaller the  $\alpha$  is, the more effective the attack is. In practice, this implies that on a finite sample of target points, attack success is frequent but not absolute.

Note that the definition of *attack effectiveness* here is general for both whitebox and blackbox attacks. In whitebox attack, the attacker is assumed to have full-knowledge about the target model including model structure and weights [1; 14; 7]; while in *blackbox attack* only the prediction probability score [45] or the

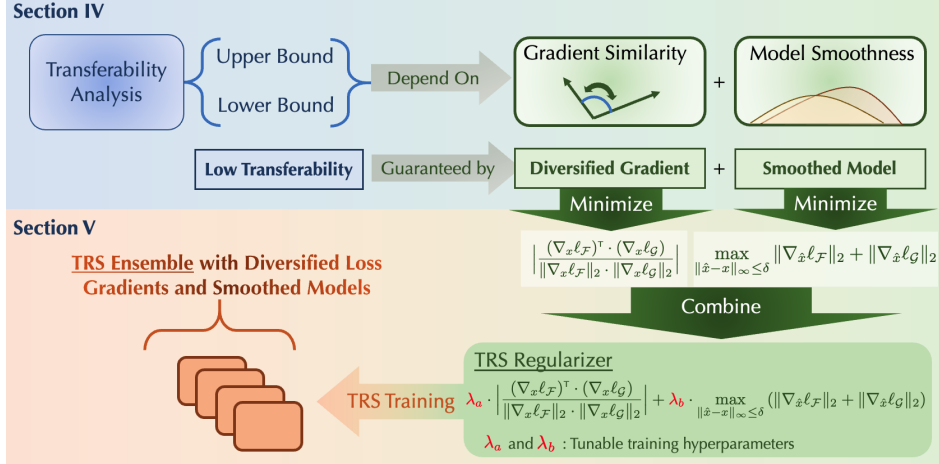


Figure 2: The overview for the Transferability Reduced Smoothing ensemble (TRS).

label decision of the model can be queried by the attacker [6]. In both types of attacks, we can use such successful attack probability to quantify the attack effectiveness naturally.

In this paper, we will focus on both targeted and untargeted adversarial effective attacks, as well as their transferability between different models (e.g.  $\mathcal{F}$  and  $\mathcal{G}$ )

### 3.2 Method Overview

An overview of our method is shown in Figure 2. We will first provide the precise definition of adversarial transferability based on our threat model in Section 4.2, and then we will present the theoretical lower and upper bounds of adversarial transferability for both untargeted and targeted attacks in Section 4. From our theoretical analysis, we find that the diversified gradients and smoother model jointly contribute to low transferability across models. Inspired by this insight, we encode these two factors into two loss terms, and propose the TRS loss to minimize the transferability between base models during training. We then propose TRS training, a progressive training approach that leverages TRS loss to consistently generate ensemble models that are diverse from others. We finally combine these models as an ensemble—TRS ensemble. The TRS ensemble is empirically evaluated against multiple strong whitebox attacks and demonstrates its robustness.

## 4 Transferability of Adversarial Perturbation

In this section, we connect adversarial transferability with different characteristics of models theoretically, which, in the next section, will allow us to explicitly minimize transferability by enforcing (or rewarding) certain properties of models. We first introduce some necessary notations and definitions, then present the theoretical analysis of adversarial transferability including its formal definition and its rigorous lower and upper bounds for both targeted and untargeted attacks.

## 4.1 Model Characteristics

Given two models  $\mathcal{F}$  and  $\mathcal{G}$ , what are the characteristics of  $\mathcal{F}$  and  $\mathcal{G}$  that have impact on transferability under a given attack strategy? Intuitively, the more similar these two classifiers are, the larger the transferability would be. However, how can we define “similar” and how can we rigorously connect it to transferability? To answer these questions, in this section we will first define the risk and empirical risk for given neural network model to measure its performance on benign test data. Then, as the deep neural networks are differentiable, we will define model similarity based on their gradients. Concretely, we define both *lower loss gradient similarity* and *upper loss gradient similarity* based on the cosine similarity between two models’ loss gradients with respect to an input. We will then derive the lower and upper bounds of transferability based on the defined model risk and similarity measures.

**Definition 3** (Model Risk). *For a given classification model  $\mathcal{F}$ , we let  $\ell_{\mathcal{F}}$  be its model-dependent loss function. Its risk is defined as  $\eta_{\mathcal{F}} = \Pr(\mathcal{F}(x) \neq y)$ ; and its empirical risk is defined as  $\xi_{\mathcal{F}} = \mathbb{E}[\ell_{\mathcal{F}}(x, y)]$ .*

As we can observe, the *risk* is exactly one minus the model’s accuracy on benign test data, while the *empirical risk* is a non-negative value that also indicates the inaccuracy. For both of them, higher value means worse performance on the benign test data. The difference is that, the risk has more intuitive meaning, while the empirical risk is differentiable and is actually used during model training in practice.

**Definition 4** (Lower Loss Gradient Similarity). *The lower loss gradient similarity  $\underline{\mathcal{S}}$  between two differentiable loss functions  $\ell_{\mathcal{F}}$  and  $\ell_{\mathcal{G}}$  is defined as:*

$$\underline{\mathcal{S}}(\ell_{\mathcal{F}}, \ell_{\mathcal{G}}) = \inf_{x \in \mathcal{X}, y \in \mathcal{Y}} \frac{\nabla_x \ell_{\mathcal{F}}(x, y) \cdot \nabla_x \ell_{\mathcal{G}}(x, y)}{\|\nabla_x \ell_{\mathcal{F}}(x, y)\|_2 \cdot \|\nabla_x \ell_{\mathcal{G}}(x, y)\|_2}.$$

The  $\underline{\mathcal{S}}(\ell_{\mathcal{F}}, \ell_{\mathcal{G}})$  is the minimum cosine similarity between the gradients of the two loss functions for an input  $x$  drawn from  $\mathcal{X}$  with the true label  $y \in \mathcal{Y}$ . Analogous with the lower loss gradient similarity, we define the upper loss gradient similarity, which is the maximum cosine similarity between the gradients of the two loss functions.

**Definition 5** (Upper Loss Gradient Similarity). *The upper loss gradient similarity  $\bar{\mathcal{S}}$  between two differentiable loss functions  $\ell_{\mathcal{F}}$  and  $\ell_{\mathcal{G}}$  is defined as:*

$$\bar{\mathcal{S}}(\ell_{\mathcal{F}}, \ell_{\mathcal{G}}) = \sup_{x \in \mathcal{X}, y \in \mathcal{Y}} \frac{\nabla_x \ell_{\mathcal{F}}(x, y) \cdot \nabla_x \ell_{\mathcal{G}}(x, y)}{\|\nabla_x \ell_{\mathcal{F}}(x, y)\|_2 \cdot \|\nabla_x \ell_{\mathcal{G}}(x, y)\|_2}$$

Besides the loss gradient similarity, in our analysis we will also show that the *model smoothness* is another key characteristic of ML models that affects the model transferability. We define the model smoothness as below.

**Definition 6** (Model Smoothness). *The model  $\mathcal{F}$  is said to be  $\beta$ -smooth if*

$$\sup_{x_1, x_2 \in \mathcal{X}, y \in \mathcal{Y}} \frac{\|\nabla_x \ell_{\mathcal{F}}(x_1, y) - \nabla_x \ell_{\mathcal{F}}(x_2, y)\|_2}{\|x_1 - x_2\|_2} \leq \beta.$$

This smoothness definition is commonly used in deep learning theory and optimization literature [5; 4], and is also named curvature bounds in certified robustness literature [49]. It could be interpreted as the Lipschitz bound for the model’s loss function gradient. We remark that *larger  $\beta$*  indicates that the model is less smoother, while *smaller  $\beta$*  means the model is smoother. Particularly, when  $\beta = 0$ , the model is linear in the input space  $\mathcal{X}$ .

## 4.2 Definition of Transferability

Based on the model characteristics we explored above, next we will ask: *Given two models, what is the natural and precise definition of adversarial transferability?*

**Definition 7** (Transferability). *Consider an adversarial instance  $\mathcal{A}_U(x)$  or  $\mathcal{A}_T(x)$  constructed against a surrogate model  $\mathcal{F}$ . With a given benign input  $x \in \mathcal{X}$ , The transferability  $T_r$  between  $\mathcal{F}$  and a target model  $\mathcal{G}$  is defined as follows (adversarial target  $y_t \in \mathcal{Y}$ ):*

- *Untargeted:*

$$T_r(\mathcal{F}, \mathcal{G}, x) = \mathbb{I}[\mathcal{F}(x) = \mathcal{G}(x) = y \wedge \mathcal{F}(\mathcal{A}_U(x)) \neq y \wedge \mathcal{G}(\mathcal{A}_U(x)) \neq y].$$

- *Targeted:*

$$T_r(\mathcal{F}, \mathcal{G}, x, y_t) = \mathbb{I}[\mathcal{F}(x) = \mathcal{G}(x) = y \wedge \mathcal{F}(\mathcal{A}_T(x)) = \mathcal{G}(\mathcal{A}_T(x)) = y_t].$$

Here we define the transferability at instance level by a predicate, where several conditions are required to satisfy. For the untargeted attack, this predicate requires that: (1) both the surrogate model and target model make correct prediction on the benign input; and (2) both of them make incorrect predictions on the adversarial input  $\mathcal{A}_U(x)$ . The  $\mathcal{A}_U(x)$  is generated via the untargeted attack against the surrogate model  $\mathcal{F}$ . For the targeted attack, this predicate requires that: (1) both the surrogate and target model make correct prediction on benign input; and (2) both output the adversarial target  $y_t \in \mathcal{Y}$  on the adversarial input  $\mathcal{A}_T(x)$ . The  $\mathcal{A}_T(x)$  is crafted against the surrogate model  $\mathcal{F}$ . Note that the predicates themselves do not require  $\mathcal{A}_U$  and  $\mathcal{A}_T$  to be explicit constructed against the surrogate model  $\mathcal{F}$ . It will be implied by attack effectiveness (definition 2) condition in following theorem's conditions.

Since the definition here is just a predicate for a specific input  $x$ , in the following analysis we will mainly use its distributional version:  $\Pr(T_r(\mathcal{F}, \mathcal{G}, x) = 1)$  and  $\Pr(T_r(\mathcal{F}, \mathcal{G}, x, y_t) = 1)$ , which measures the overall average transferability over a finite number of inputs for a given classification task.

This definition of transferability directly encodes the probability that the crafted adversarial examples against a surrogate model transfer to the target model. In contrast, the previous work (e.g., [14]) usually defines the transferability over the loss functions  $\ell_{\mathcal{F}}$  and  $\ell_{\mathcal{G}}$ , which actually draws an indirect connection with the observed transferability phenomenon.

## 4.3 Lower Bound of Transferability

Based on the general definition of transferability, in this section we will analyze how to lower bound the transferability for both targeted and untargeted attacks, and what are the corresponding sufficient conditions.

**Theorem 1** (Lower Bound on Targeted Attack Transferability). *Assume both models  $\mathcal{F}$  and  $\mathcal{G}$  are  $\beta$ -smooth. Let  $\mathcal{A}_T$  be an  $(\alpha, \mathcal{F})$ -effective targeted attack with perturbation ball  $\|\delta\|_2 \leq \epsilon$  and target label  $y_t \in \mathcal{Y}$ . The transferability can be lower bounded by*

$$\Pr(T_r(\mathcal{F}, \mathcal{G}, x, y_t) = 1) \geq (1 - \alpha) - (\eta_{\mathcal{F}} + \eta_{\mathcal{G}}) - \frac{\epsilon(1 + \alpha) + c_{\mathcal{F}}(1 - \alpha)}{c_{\mathcal{G}} + \epsilon} - \frac{\epsilon(1 - \alpha)}{c_{\mathcal{G}} + \epsilon} \sqrt{2 - 2\mathcal{S}(\ell_{\mathcal{F}}, \ell_{\mathcal{G}})},$$

where

$$c_{\mathcal{F}} = \max_{x \in \mathcal{X}} \frac{\min_{y \in \mathcal{Y}} \ell_{\mathcal{F}}(\mathcal{A}_T(x), y) - \ell_{\mathcal{F}}(x, y_t) + \beta\epsilon^2/2}{\|\nabla_x \ell_{\mathcal{F}}(x, y_t)\|_2}, \quad c_{\mathcal{G}} = \min_{x \in \mathcal{X}} \frac{\min_{y \in \mathcal{Y}} \ell_{\mathcal{G}}(\mathcal{A}_T(x), y) - \ell_{\mathcal{G}}(x, y_t) - \beta\epsilon^2/2}{\|\nabla_x \ell_{\mathcal{G}}(x, y_t)\|_2}.$$

Here  $\eta_{\mathcal{F}}, \eta_{\mathcal{G}}$  are the risks of models  $\mathcal{F}$  and  $\mathcal{G}$  respectively.

Similarly, we have the following theorem for untargeted attack.

**Theorem 2** (Lower Bound on Untargeted Attack Transferability). *Assume both models  $\mathcal{F}$  and  $\mathcal{G}$  are  $\beta$ -smooth. Let  $\mathcal{A}_U$  be an  $(\alpha, \mathcal{F})$ -effective untargeted attack with perturbation ball  $\|\delta\|_2 \leq \epsilon$ . The transferability can be lower bounded by*

$$\Pr(T_r(\mathcal{F}, \mathcal{G}, x) = 1) \geq (1 - \alpha) - (\eta_{\mathcal{F}} + \eta_{\mathcal{G}}) - \frac{\epsilon(1 + \alpha) - c_{\mathcal{F}}(1 - \alpha)}{\epsilon - c_{\mathcal{G}}} - \frac{\epsilon(1 - \alpha)}{\epsilon - c_{\mathcal{G}}} \sqrt{2 - 2\underline{\mathcal{S}}(\ell_{\mathcal{F}}, \ell_{\mathcal{G}})},$$

where

$$c_{\mathcal{F}} = \min_{(x, y) \in \text{supp}(\mathcal{D})} \frac{\min_{y' \in \mathcal{Y}: y' \neq y} \ell_{\mathcal{F}}(\mathcal{A}_U(x), y') - \ell_{\mathcal{F}}(x, y) - \beta\epsilon^2/2}{\|\nabla_x \ell_{\mathcal{F}}(x, y)\|_2}, \quad c_{\mathcal{G}} = \max_{(x, y) \in \text{supp}(\mathcal{D})} \frac{\min_{y' \in \mathcal{Y}: y' \neq y} \ell_{\mathcal{G}}(\mathcal{A}_U(x), y') - \ell_{\mathcal{G}}(x, y) + \beta\epsilon^2/2}{\|\nabla_x \ell_{\mathcal{G}}(x, y)\|_2}.$$

Here  $\eta_{\mathcal{F}}$  and  $\eta_{\mathcal{G}}$  are the risks of models  $\mathcal{F}$  and  $\mathcal{G}$  respectively. The  $\text{supp}(\mathcal{D})$  is the support of benign data distribution, i.e.,  $x$  is the benign data and  $y$  is its associated true label.

*Proof (Sketch).* The main challenge for lower bounding transferability is to connect the misclassification of  $\mathcal{F}$  to the misclassification of  $\mathcal{G}$  purely using their loss gradient similarities. We first use a Taylor expansion to introduce the gradient terms and eliminate higher-order terms by  $\beta$ -bounded Hessian matrix eigenvalues. We then connect the gradient terms with the misclassification probability. To do so, we prove and apply Lemma 7 (Appendix B) which relates the dot product with cosine similarities of the loss gradients. Finally, we calculate the upper bound of the expectation of  $\delta \cdot \frac{\nabla_x \ell_{\mathcal{G}}(x, y_t)}{\|\nabla_x \ell_{\mathcal{G}}(x, y_t)\|_2}$ , and use Markov's inequality to derive the misclassification probability of  $\mathcal{G}$ , which complete the proof. The full proof of this result can be found in Appendix B.  $\square$

In the above theorems, we use *risk*  $\eta_{\mathcal{F}}$  and  $\eta_{\mathcal{G}}$  to represent the model risk. Compared with *empirical risk*, the *risk* is directly related to the model inaccuracy, and thus more informative and provides intuitive understanding. It is also possible to derive the lower bound based on the empirical risk which will be of slightly more complicated form, and we will not discuss it in details here.

**Implications.** In both Theorems 1 and 2, the only term which correlates both  $\mathcal{F}$  and  $\mathcal{G}$  is  $\underline{\mathcal{S}}(\ell_{\mathcal{F}}, \ell_{\mathcal{G}})$ , while all other terms depend on individual models  $\mathcal{F}$  or  $\mathcal{G}$ . Thus, we can view all other terms as constant.

Since  $\beta$  is small compared with the perturbation radius  $\epsilon$  and the gradient magnitude  $\|\nabla_x \ell_{\mathcal{G}}\|_2$  in the denominator is relatively large, the quantity  $c_{\mathcal{G}}$  is small. Moreover,  $1 - \alpha$  is large since the attack is typically effective against  $\mathcal{F}$  by definition. Thus, both  $\Pr(T_r(\mathcal{F}, \mathcal{G}, x, y_t) = 1)$  and  $\Pr(T_r(\mathcal{F}, \mathcal{G}, x) = 1)$  have the form  $C - k\sqrt{1 - \underline{\mathcal{S}}(\ell_{\mathcal{F}}, \ell_{\mathcal{G}})}$ , where  $C$  and  $k$  are both positive constants. We can easily observe the positive correlation between the loss gradients similarity  $\underline{\mathcal{S}}(\ell_{\mathcal{F}}, \ell_{\mathcal{G}})$ , and lower bound of adversarial transferability  $T_r(\mathcal{F}, \mathcal{G}, x, y_t)$  or  $T_r(\mathcal{F}, \mathcal{G}, x)$ .

In the meantime, note that when  $\beta$  increases (i.e., model becomes less smooth), in the transferability lower bound  $C - k\sqrt{1 - \underline{\mathcal{S}}(\ell_{\mathcal{F}}, \ell_{\mathcal{G}})}$ , the  $C$  decreases and  $k$  increase. As a result, both lower bounds in Theorems 1 and 2 decrease, which implies that when model becomes less smoother, the transferability lower bounds become looser for both targeted and untargeted attacks. In other words, *when the model becomes smoother, the correlation between loss gradients similarity and lower bound of transferability becomes stronger*, which motivates us to improve the model smoothness to increase the effect of constraining loss gradients similarity. The theorems formalize the intuition that *low risk classifiers would potentially have high transferability* if their loss gradients similarity and smoothness are sufficiently high as observed in exiting work (cf. [14]).

Though it seems pessimistic given the lower bound of transferability, we would ask another question: *Is it possible to upper bound the transferability given additional constraints?*

## 4.4 Upper Bound of Transferability For Smoothed Classifiers

Suppose we have two models  $\mathcal{F}$  and  $\mathcal{G}$ , then for any targeted adversarial attack, we can upper bound the transferability of the two models by constraining their loss gradients similarity and model smoothness as shown in the following theorems.

**Theorem 3** (Upper Bound on Targeted Attack Transferability). *Assume both models  $\mathcal{F}$  and  $\mathcal{G}$  are  $\beta$ -smooth with gradient magnitude bounded by  $B$ , i.e.,  $\|\nabla_x \ell_{\mathcal{F}}(x, y)\| \leq B$  and  $\|\nabla_x \ell_{\mathcal{G}}(x, y)\| \leq B$  for any  $x \in \mathcal{X}, y \in \mathcal{Y}$ . Let  $\mathcal{A}_T$  be an  $(\alpha, \mathcal{F})$ -effective targeted attack with perturbation ball  $\|\delta\|_2 \leq \epsilon$  and target label  $y_t \in \mathcal{Y}$ . The transferability can be upper bounded by*

$$\Pr(T_r(\mathcal{F}, \mathcal{G}, x, y_t) = 1) \leq \frac{\xi_{\mathcal{F}} + \xi_{\mathcal{G}}}{\ell_{\min} - \epsilon B \left(1 + \sqrt{\frac{1+\bar{S}(\ell_{\mathcal{F}}, \ell_{\mathcal{G}})}{2}}\right) - \beta \epsilon^2},$$

where

$$\ell_{\min} = \min_{x \in \mathcal{X}} (\ell_{\mathcal{F}}(x, y_t), \ell_{\mathcal{G}}(x, y_t)).$$

Here  $\xi_{\mathcal{F}}$  and  $\xi_{\mathcal{G}}$  are the empirical risks of models  $\mathcal{F}$  and  $\mathcal{G}$  respectively, defined relative to a differentiable loss.

Similarly, we can upper bound the transferability of untargeted attacks as below.

**Theorem 4** (Upper Bound on Untargeted Attack Transferability). *Assume both models  $\mathcal{F}$  and  $\mathcal{G}$  are  $\beta$ -smooth with gradient magnitude bounded by  $B$ , i.e.,  $\|\nabla_x \ell_{\mathcal{F}}(x, y)\| \leq B$  and  $\|\nabla_x \ell_{\mathcal{G}}(x, y)\| \leq B$  for any  $x \in \mathcal{X}, y \in \mathcal{Y}$ . Let  $\mathcal{A}_U$  be an  $(\alpha, \mathcal{F})$ -effective untargeted attack with perturbation ball  $\|\delta\|_2 \leq \epsilon$ . The transferability can be upper bounded by*

$$\Pr(T_r(\mathcal{F}, \mathcal{G}, x) = 1) \leq \frac{\xi_{\mathcal{F}} + \xi_{\mathcal{G}}}{\ell_{\min} - \epsilon B \left(1 + \sqrt{\frac{1+\bar{S}(\ell_{\mathcal{F}}, \ell_{\mathcal{G}})}{2}}\right) - \beta \epsilon^2},$$

where

$$\ell_{\min} = \min_{\substack{x \in \mathcal{X}, y' \in \mathcal{Y}: \\ (x, y) \in \text{supp}(\mathcal{D}), y' \neq y}} (\ell_{\mathcal{F}}(x, y'), \ell_{\mathcal{G}}(x, y')).$$

Here  $\xi_{\mathcal{F}}$  and  $\xi_{\mathcal{G}}$  are the empirical risks of models  $\mathcal{F}$  and  $\mathcal{G}$  respectively, defined relative to a differentiable loss. The  $\text{supp}(\mathcal{D})$  is the support of benign data distribution, i.e.,  $x$  is the benign data and  $y$  is its associated true label.

*Proof (Sketch).* When the gradient vectors are very dissimilar, any perturbation will be disadvantageous for the adversary on at least one of the models. We formalize this observation to Lemma 8 (in the Appendix). Then, we take a Taylor expansion on the loss function at  $(x, y)$  to approximate the adversarial's crafted input  $(\mathcal{A}(x), y)$  and link the gradient with the misclassification loss. Using the fact that the attack direction will be dissimilar with at least one of the model gradients, we can upper bound the probability of transferability using Markov's inequality on the loss function. A full proof can be found in Appendix C.  $\square$

**Implications.** In both Theorems 3 and 4, we can observe that along with the increase of  $\bar{S}(\ell_{\mathcal{F}}, \ell_{\mathcal{G}})$ , the denominator decreases and henceforth the upper bound increases. Therefore,  $\bar{S}(\ell_{\mathcal{F}}, \ell_{\mathcal{G}})$ —upper loss gradient similarity and the upper bound of  $T_r(\mathcal{F}, \mathcal{G}, x, y_t)$  or  $T_r(\mathcal{F}, \mathcal{G}, x)$  are positively correlated. The tendency is the same as that in the lower bound. This establishes that the gradient similarity between models is highly correlated with transferability. (Note that  $\alpha$  does not appear in upper bounds since only completely successful attacks ( $\alpha = 0\%$ ) needs to be considered here to upper bound the transferability.)

Meanwhile, when  $\beta$  increases (i.e., model becomes less smooth), the transferability upper bound also increases, which implies that when the model becomes smoother (i.e.,  $\beta$  decreases), the transferability upper bound

decreases and becomes tighter, which motivates us to improve the model smoothness to better reflect the effect of constraining gradient similarity. We remark that a new term, the magnitude of gradient  $B$ , appears in the upper bounds. The smaller the magnitude of gradient  $B$  implies larger denominator and thus smaller transferability. This aligns with previous findings [14], and our proposed TRS will also optimize the model toward smaller  $B$  for robustness purpose.

**Impact of model smoothness  $\beta$ .** Combined with the transferability lower bound, we find that smaller  $\beta$  leads to increased lower and decreased upper bounds, that is, tighter transferability bounds. It implies that when  $\beta$  becomes smaller (smoother model), there is less uncertainty about transferability, i.e., the correlation between loss gradients similarity and transferability becomes stronger. As a result, based on theoretical analysis it is possible to increase model smoothness (decrease  $\beta$ ), and at the same time constraining gradient similarity to reduce model transferability to improve ensemble robustness (only constraining the loss gradients similarity is not enough which confirms the empirical observations in existing work [25] and our experiments in Section 6).

## 5 Improving Ensemble Robustness via Transferability Minimization

Built upon our theoretical analysis on adversarial transferability, we propose a lightweight yet effective robust ensemble training approach to reduce the transferability among base models by enforcing the *model smoothness* and *low loss gradient similarities* at the same time. In particular, inspired by the factors that affect the upper bound of transferability, we develop Transferability Reduced Smooth (TRS) ensemble training approach to reduce adversarial transferability among base models, and thus enhance the ensemble robustness.

### 5.1 TRS Regularizer

In practice, to ensure the trained model smoothness, regularizing the model directly is challenging. Luckily, derived from deep learning theory and optimization [16; 41], succinct  $\ell_2$  regularization on the gradient terms  $\|\nabla_x \ell_{\mathcal{F}}\|_2$  and  $\|\nabla_x \ell_{\mathcal{G}}\|_2$  can reduce the magnitude of gradients and thus improve *model smoothness*. An intuitive explanation is that, the  $\ell_2$  regularization on the gradient terms reduces the magnitude of model's weights, thus limits its changing rate when non-linear activation functions are applied to the neural network model. However, in the real evaluation we find that only regularizing the loss gradient magnitude with  $\ell_2$  norm directly is not enough, since a vanilla  $\ell_2$  regularizer such as  $\|\nabla_x \ell_{\mathcal{F}}\|_2$  will only focus on the local region at data point  $x$ , while it is required to ensure the model smoothness over a large decision regime so as to control the adversarial transferability based on our analysis of its upper bound.

To address this challenges, we propose a min-max framework to search for the “support” instances which maximizes the *model smoothness loss* first, and then focus on minimizing the loss on the neighborhood regions of the decision boundary. In particular, we compute the model smoothness loss as below.

$$\mathcal{L}_{\text{smooth}}(\mathcal{F}, \mathcal{G}, x, \delta) = \max_{\|\hat{x} - x\|_\infty \leq \delta} \|\nabla_{\hat{x}} \ell_{\mathcal{F}}\|_2 + \|\nabla_{\hat{x}} \ell_{\mathcal{G}}\|_2$$

where  $\delta$  refers to the radius of the  $\ell_\infty$  ball around instance  $x$  within which we aim to ensure our model to be smooth. In practice, we leverage the Projection Gradient Descent (PGD) procedure to search for support instances  $\hat{x}$  for optimization. We will compare the ensemble robustness of the proposed model smoothness approach with the naive baseline as directly applying the  $\ell_2$  loss on each model loss gradient for model smoothing (i.e. Cos- $\ell_2$ ) in Section 6.

Given trained “smoothed” base models, we will decrease the model loss gradient similarity to reduce the overall adversarial transferability between base models. Among various metrics which measure the similarity between the loss gradients of base model  $\mathcal{F}$  and  $\mathcal{G}$ , we find that the vanilla cosine similarity metric, which is

also used in [25], may lead to certain concerns. By minimizing the cosine similarity between  $\nabla_x \ell_{\mathcal{F}}$  and  $\nabla_x \ell_{\mathcal{G}}$ , the optimal case implies  $\nabla_x \ell_{\mathcal{F}} = -\nabla_x \ell_{\mathcal{G}}$ , which means two models have contradictory (rather than diverse) performance on instance  $x$  and thus results in turbulent model functionality. Based on this consideration, we choose the absolute value of cosine similarity between  $\nabla_x \ell_{\mathcal{F}}$  and  $\nabla_x \ell_{\mathcal{G}}$  as *similarity loss*  $\mathcal{L}_{\text{sim}}$  while its optimal case implies orthogonal loss gradient vectors. For simplification, we will always use *gradient similarity* as the absolute value of the gradient cosine similarity in our later description and evaluation.

Inspired by the principles we mentioned above, we define the TRS regularizer term  $\mathcal{L}_{\text{TRS}}$  between model pair  $(\mathcal{F}, \mathcal{G})$  on input  $x$  as the following:

$$\begin{aligned}\mathcal{L}_{\text{TRS}}(\mathcal{F}, \mathcal{G}, x, \delta) &= \lambda_a \cdot \mathcal{L}_{\text{sim}} + \lambda_b \cdot \mathcal{L}_{\text{smooth}} \\ &= \lambda_a \cdot \left| \frac{(\nabla_x \ell_{\mathcal{F}})^\top (\nabla_x \ell_{\mathcal{G}})}{\|\nabla_x \ell_{\mathcal{F}}\|_2 \cdot \|\nabla_x \ell_{\mathcal{G}}\|_2} \right| + \lambda_b \cdot \left[ \max_{\|\hat{x} - x\|_\infty \leq \delta} \|\nabla_{\hat{x}} \ell_{\mathcal{F}}\|_2 + \|\nabla_{\hat{x}} \ell_{\mathcal{G}}\|_2 \right]\end{aligned}$$

Here  $\nabla_x \ell_{\mathcal{F}}, \nabla_x \ell_{\mathcal{G}}$  refer to the loss gradient vectors of base models  $\mathcal{F}$  and  $\mathcal{G}$  on input  $x$ , and  $\lambda_a, \lambda_b$  the weight balancing parameters.

We will systematically show that the introduction of the local min-max training and the absolute value of the cosine similarity between the model loss gradients significantly improve the generalization of model smoothness with negligible performance drop on model benign accuracy, as well as reduce the adversarial transferability among base models. We will provide detailed empirical evaluation on the ensemble robustness and adversarial transferability in Section 6.

## 5.2 TRS Training

We integrate the proposed TRS regularizer with the standard ensemble training loss, such as Ensemble Cross-Entropy (ECE) loss, to maintain both ensemble model's classification utility and robustness by varying the balancing parameter  $\lambda_a$  and  $\lambda_b$ . Specifically, for an ensemble model consisting of  $N$  base models  $\{\mathcal{F}_i\}$ , given an input  $(x, y)$ , our final training loss train is defined as:

$$\mathcal{L}_{\text{train}} = \frac{1}{N} \sum_{i=1}^N \mathcal{L}_{\text{CE}}(\mathcal{F}_i(x), y) + \frac{2}{N(N-1)} \sum_{i=1}^N \sum_{j=i+1}^N \mathcal{L}_{\text{TRS}}(\mathcal{F}_i, \mathcal{F}_j, x, \delta)$$

where  $\mathcal{L}_{\text{CE}}(\mathcal{F}_i(x), y)$  refers to the cross-entropy loss between  $\mathcal{F}_i(x)$  the output vector of model  $\mathcal{F}_i$  given  $x$ , and the ground-truth label  $y$ . The weight of  $\mathcal{L}_{\text{TRS}}$  regularizer could be adjusted by the tuning  $\lambda_a$  and  $\lambda_b$  internally.

The detailed TRS training algorithm for one epoch is illustrated in Algorithm 1. We apply the mini-batch training strategy and train the TRS ensemble for  $M$  epochs ( $M = 120$  for MNIST and  $M = 200$  for CIFAR-10) in our experiments. To decide the  $\delta$  within the local min-max procedure, we use the **Warm-up** strategy by linearly increasing the local  $\ell_\infty$  ball's radius  $\delta$  from small initial  $\delta_0$  to the final  $\delta_M$  along with the increasing of training epochs. Due to the space limitation, We put more training details into the Appendix D.

## 6 Experimental Evaluation

In this section, we evaluate the robustness of the proposed TRS-ensemble model under both whitebox and blackbox attack settings, and compare with the state-of-the-art ensemble learning approaches. In addition, we evaluate the adversarial transferability among base models within an ensemble and empirically show that the TRS regularizer can indeed reduce transferability effectively. We also conduct extensive ablation studies to explore the effectiveness of different loss terms in TRS, as well as visualize the trained decision boundaries of a range of ensemble models to provide intuition on the model properties. We will open source

---

**Algorithm 1** TRS training framework in epoch  $m$  for an ensemble with  $N$  base models  $\{\mathcal{F}_i\}$ , with the total number training epochs  $M$ .

---

```

1:  $\delta_m \leftarrow \delta_0 + (\delta_M - \delta_0) \cdot m/M$ 
2: for  $b = 1, \dots, B$  do
3:    $(x, y) \leftarrow$  training instances from  $b$ -th mini-batch
4:   for  $i = 1, \dots, N$  do
5:     for  $j = i + 1, \dots, N$  do
6:        $\mathcal{L}_{\text{Reg}} \leftarrow \mathcal{L}_{\text{Reg}} + \mathcal{L}_{\text{TRS}}(\mathcal{F}_i, \mathcal{F}_j, x, \delta_m)$ 
7:     end for
8:   end for
9:   for  $i = 1, \dots, N$  do
10:     $\mathcal{L}_{\text{ECE}} \leftarrow \mathcal{L}_{\text{ECE}} + \mathcal{L}_{\text{CE}}(\mathcal{F}_i(x), y)$ 
11:  end for
12:   $\mathcal{L}_{\text{Reg}} \leftarrow \mathcal{L}_{\text{Reg}} / \binom{N}{2}$ 
13:   $\mathcal{L}_{\text{ECE}} \leftarrow \mathcal{L}_{\text{ECE}} / N$ 
14:  for  $i = 1, \dots, N$  do
15:     $\nabla_{\mathcal{F}_i} \leftarrow \nabla_{\mathcal{F}_i} [\mathcal{L}_{\text{ECE}} + \mathcal{L}_{\text{Reg}}]$ 
16:     $\mathcal{F}_i \leftarrow \mathcal{F}_i - lr \cdot \nabla_{\mathcal{F}_i}$ 
17:  end for
18: end for

```

---

our implementation for reproducibility purpose and provide a large-scale benchmark for the community of robustness and ensemble learning.

## 6.1 Experimental Setup

**Datasets.** We conduct our experiments on widely-used image datasets including MNIST, CIFAR-10, and CIFAR-100 [32; 29]. MNIST [32] is a gray-scale hand-written digits dataset with 60,000 training images and 10,000 testing images with label from 0 to 9. CIFAR-10 [29] consists of 10 categorical colour images with 5,000 training images and 1,000 testing images on each class. CIFAR-100 [29], which is similar to CIFAR-10, consists of 100 classes colour images with 500 training and 100 testing images for each class.

**Baseline ensemble approaches.** We mainly consider the standard vanilla ensemble training, as well as the state-of-the-art robust ensemble methods that claim to be resilient against adversarial attacks, as the baseline methods to compare with the proposed TRS ensemble. We introduce these baseline ensemble methods as below, which all aim to promote the diversity between base models within an ensemble in different ways.

- **Boosting** [39; 48] is a natural way of model ensemble training, which builds different weak learners in a sequential manner improving diversity in handling different task partitions. Here we consider two variants of boosting algorithms: 1) **AdaBoost** [22], where the final prediction will be the weighted average of all the weak learners: weight  $\alpha_i$  for  $i$ -th base model is decided by the accumulated error  $e_i$  as  $\alpha_i = \log \frac{1-e_i}{e_i} + \log(K-1)$ . Here  $K$  refers to the number of categories in a classification task. As we can see, higher weight will be placed on stronger learners. 2) **GradientBoost** [19], which is a general ensemble training method by identifying weaker learners based on gradient information and generating the ensemble by training base models step by step with diverse learning orientations within pseudo-residuals  $r = -\frac{\partial \ell(f(x), y)}{\partial f(x)}$  computed from the current ensemble model  $f$  on input  $x$  with ground truth label  $y$ .
- **CKAE** [28] develops diverse ensembles based on CKA measurement, which is recently shown to be effective to measure the orthogonality between representations. For two representations  $K$  and  $L$ ,  $\text{CKA}(K, L) = \frac{\text{HSIC}(K, L)}{\sqrt{\text{HSIC}(K, K)\text{HSIC}(L, L)}}$ ,  $\text{HSIC}(K, L) = \frac{1}{(n-1)^2} \text{tr}(KHLH)$ , where  $n$  is the number of samples and  $H$  the

centering matrix. For an ensemble consisting of base models  $\{\mathcal{F}_i\}$ , we regard the representation of  $\mathcal{F}_i$  as its loss gradient vectors on batch samples and then minimize pair-wise CKA between base models  $\mathcal{F}_i, \mathcal{F}_j$ 's representations to encourage ensemble diversity.

- **ADP** [42] is proposed recently as an effective regularization-based training method to reduce adversarial transferability among base models within an ensemble by maximizing the volume spanned by base models' non-maximal output vectors. Specifically, for a ensemble consisting of base models  $\{\mathcal{F}_i\}$  and input  $x$  with ground truth label  $y$ , the ADP regularizer is defined as  $\mathcal{L}_{\text{ADP}}(x, y) = \alpha \cdot H(\text{mean}(\{\mathcal{F}_i(x)\})) + \beta \cdot \log(\mathbb{E}\mathbb{D})$ , where  $H(\cdot)$  is the Shannon Entropy Loss and  $\mathbb{E}\mathbb{D}$  the square of the spanned volume. Nevertheless, the ADP ensemble has been shown to be vulnerable against attacks that run for enough iterations until converged [53]. We will also discuss this similar observation in our empirical robustness evaluation.
- **GAL** [25] promotes the diverse properties of the ensemble model by only minimizing the actual cosine similarities between pair-wise base models' loss gradient vectors. For  $N$  base models  $\{\mathcal{F}_i\}$  within an ensemble and input  $x$  with ground truth label  $y$ , the GAL regularizer is defined as:  

$$\mathcal{L}_{\text{GAL}} = \log(\sum_{1 \leq i < j \leq N} \exp(CS(\nabla_x \ell_{\mathcal{F}_i}, \nabla_x \ell_{\mathcal{F}_j}))$$
 where  $CS(\cdot, \cdot)$  refers to the actual cosine similarity measurement and  $\nabla_x \ell_{\mathcal{F}_i}$  the loss gradient of base model  $\mathcal{F}_i$  on  $x$ . It could serve as a baseline to empirically verify our theoretical analysis: based on similar model loss gradient similarity, the smoother the base models are, the less transferable they are.
- **DVERGE** [57] reduces the transferability among base models by utilizing Cross-Adversarial-Training: For a ensemble consisting of base models  $\{\mathcal{F}_i\}$  and input  $x$  with ground truth label  $y$ , each base model  $\mathcal{F}_i$  is trained with the non-robust feature instances [24] generated against another base model. Specifically, DVERGE minimizes  $\sum_{j \neq i} \ell(\mathcal{F}_i(x'_{\mathcal{F}_j}(x_s, x)), y_s)$  for every  $\mathcal{F}_i$  iteratively, where  $x'_{\mathcal{F}_j}(x_s, x)$  represents the non-robust features against  $\mathcal{F}_j$  based on the randomly chosen input  $(x_s, y_s)$ .  $\ell(\cdot, \cdot)$  is the cross-entropy loss function. DVERGE, which serves as the strongest baseline robust ensemble approach, has achieved the state-of-the-art ensemble robustness and low adversarial transferability among base models.

**Training details.** In our experiments, we employ the widely-used ResNet-20 network [23] as base models' architecture and considered the ensemble consisting of **3 base models** always. For all the baseline ensemble models mentioned above, we adapt the same training parameter and reproduced the results as in the original paper. In TRS ensemble training, we follow our described training algorithm by combining TRS regularizer  $\mathcal{L}_{\text{TRS}}$  with Ensemble CrossEntropy (ECE) Loss and varying the weight parameter  $\lambda_a, \lambda_b$ . We set  $\lambda_a = 100, \lambda_b = 2.5$  and  $\delta_0 = 0.1, \delta_M = 0.3$  for MNIST, and  $\lambda_a = 20, \lambda_b = 2.5$  and  $\delta_0 = 0.01, \delta_M = 0.03$  for both CIFAR-10 and CIFAR-100 to balance the overall robustness and accuracy. We apply 5-steps  $\ell_\infty$  PGD optimization with step size equals to  $\delta_m/4$  to search for  $\hat{x}$ . We also explore other hyper-parameter settings and obtain similar results as shown in Appendix F.

**Whitebox robustness evaluation.** We consider the following adversarial attacks to measure ensembles' whitebox robustness. Here we define  $(x, y)$  to be the input  $x$  with label  $y$  and  $x^A$  to be the notion of adversarial example generated from  $x$ .  $\ell(\mathcal{F}(x), y)$  refers to the loss between model output  $\mathcal{F}(x)$  and label  $y$ , and  $\epsilon$  is the  $\ell_\infty$  perturbation magnitude bound for different attacks.

- *Fast Gradient Sign Method* (FGSM) [20] is a simple yet effective attack strategy which generates adversarial example  $x^A = x + \nu$  by assigning  $\nu = \epsilon \cdot \text{sgn}(\nabla_x \ell(\mathcal{F}(x), y))$ .
- *Basic Iterative Method* (BIM) [38] is an iterative attack method which adds adversarial perturbations step by step:  $x_{i+1} = \text{clip}(x_i + \alpha \cdot \nabla_{x_i} \ell(\mathcal{F}(x_i), y))$ , with initial starting point  $x_0 = x$ . Function  $\text{clip}(\cdot)$  projects the perturbed instance back to the  $\ell_\infty$  ball within the perturbation range  $\epsilon$ , and  $\alpha$  refers to the step size.
- *Momentum Iterative Method* (MIM) [15] can be regarded as the variant of BIM by utilizing the gradient momentum during the iterative attack procedure. Within iteration  $i + 1$ , we update new gradient as  $g_{i+1} = \mu g_i + \frac{\ell(\mathcal{F}(x_i), y)}{\|\nabla_x \ell(\mathcal{F}(x_i), y)\|_1}$  and set  $x_{i+1} = \text{clip}(x_i + \alpha \cdot g_{i+1})$  while  $\mu$  refers to the momentum coefficient and  $\alpha$  the step size.

Table 1: Robust accuracy (%) of different approaches against various whitebox attacks on MNIST dataset.

MNIST	para.	AdaBoost	GradientBoost	CKAE	ADP	GAL	DVERGE	Cos-only	Cos- $\ell_2$	TRS
FGSM	$\epsilon = 0.1$	70.2	73.2	72.6	71.7	35.7	<b>95.8</b>	66.2	91.2	95.6
	$\epsilon = 0.2$	39.4	34.2	42.5	20.0	7.8	91.6	30.7	72.5	<b>91.7</b>
BIM (50)	$\epsilon = 0.1$	2.6	2.4	4.2	7.7	4.6	74.9	0.4	76.2	<b>93.3</b>
	$\epsilon = 0.15$	0.0	0.2	0.4	0.1	2.5	47.7	0.0	47.9	<b>85.7</b>
PGD (50)	$\epsilon = 0.1$	1.9	1.5	1.4	4.5	4.1	69.2	0.0	73.4	<b>93.0</b>
	$\epsilon = 0.15$	0.0	0.0	0.5	1.0	0.6	28.8	0.0	30.2	<b>85.1</b>
MIM (50)	$\epsilon = 0.1$	1.9	1.6	1.2	13.8	0.8	75.3	0.4	74.1	<b>92.9</b>
	$\epsilon = 0.15$	0.0	0.1	0.3	1.0	0.2	44.6	0.0	35.5	<b>85.1</b>
CW	$c = 0.1$	81.2	80.5	83.4	97.9	97.4	97.3	85.6	89.2	<b>98.1</b>
	$c = 1.0$	66.3	65.8	69.5	90.1	68.3	79.2	58.6	54.4	<b>92.6</b>
EAD	$c = 5.0$	0.2	0.1	0.1	2.2	0.2	0.0	4.1	6.9	<b>23.3</b>
	$c = 10.0$	0.0	0.0	0.0	0.0	0.2	0.0	0.5	0.8	<b>1.4</b>
APGD-DLR	$\epsilon = 0.1$	0.5	0.2	0.5	2.1	1.9	65.4	0.0	70.6	<b>92.1</b>
	$\epsilon = 0.15$	0.0	0.0	0.1	0.5	0.2	27.4	0.0	26.3	<b>83.4</b>
APGD-CE	$\epsilon = 0.1$	0.2	0.2	0.1	1.4	1.2	63.2	0.0	69.8	<b>91.7</b>
	$\epsilon = 0.15$	0.0	0.0	0.1	0.4	0.2	26.1	0.0	25.4	<b>82.8</b>

Table 2: Robust accuracy (%) of different approaches against various whitebox attacks on CIFAR-10 dataset.

CIFAR-10	para.	AdaBoost	GradientBoost	CKAE	ADP	GAL	DVERGE	Cos-only	Cos- $\ell_2$	TRS
FGSM	$\epsilon = 0.02$	28.2	30.4	34.1	58.8	19.2	<b>63.8</b>	56.1	35.8	36.8
	$\epsilon = 0.04$	15.4	15.2	18.5	39.4	12.6	<b>53.4</b>	35.0	25.9	17.4
BIM (50)	$\epsilon = 0.01$	4.2	4.4	5.1	13.8	13.0	39.1	0.0	17.1	<b>47.3</b>
	$\epsilon = 0.02$	0.2	0.1	0.2	0.9	2.5	13.0	0.0	1.2	<b>15.9</b>
PGD (50)	$\epsilon = 0.01$	2.1	1.9	1.9	9.0	8.3	37.1	0.0	15.7	<b>47.3</b>
	$\epsilon = 0.02$	0.0	0.0	0.2	0.1	0.6	10.5	0.0	0.5	<b>15.5</b>
MIM (50)	$\epsilon = 0.01$	2.3	1.9	2.0	18.7	10.3	40.7	0.0	18.1	<b>47.9</b>
	$\epsilon = 0.02$	0.1	0.0	0.1	1.7	0.8	14.4	0.0	0.5	<b>17.6</b>
CW	$c = 0.01$	36.2	35.2	35.4	55.8	66.3	75.1	36.6	67.3	<b>75.8</b>
	$c = 0.1$	18.4	26.2	23.0	25.9	28.3	57.4	17.6	30.7	<b>58.2</b>
EAD	$c = 1.0$	0.2	0.0	0.0	9.0	0.0	0.2	0.0	0.0	<b>16.8</b>
	$c = 5.0$	0.0	0.0	0.0	0.0	0.0	0.0	0.0	0.0	<b>0.5</b>
APGD-DLR	$\epsilon = 0.01$	1.2	0.9	1.1	5.5	2.2	37.6	0.0	16.1	<b>47.3</b>
	$\epsilon = 0.02$	0.0	0.0	0.0	0.2	0.0	10.2	0.0	0.5	<b>15.3</b>
APGD-CE	$\epsilon = 0.01$	0.9	0.2	0.4	3.9	1.6	37.5	0.0	15.9	<b>45.8</b>
	$\epsilon = 0.02$	0.0	0.0	0.0	0.1	0.0	10.2	0.0	0.5	<b>14.9</b>

- *Projected Gradient Descent* (PGD) [38] can be regarded as the variant of BIM by sampling  $x_0$  randomly within the  $\ell_p$  ball around  $x$  within radius  $\epsilon$ . After initialization, it follows the standard BIM procedure by setting  $x_{i+1} = \text{clip}(x_i + \alpha \cdot \nabla_{x_i} \ell(\mathcal{F}(x_i), y))$  on  $i$ -th attack iteration.
- *Auto-PGD* (APGD) [13] is a step-size free variant of PGD by configuring the step-size according to the overall iteration budgets and the progress of the current attack. Here we consider APGD-CE and APGD-DLR attack which use CrossEntropy (CE) and Difference of Logits Ratio (DLR) [13] loss as their loss function correspondingly.
- *Carlini & Wanger Attack* (CW) [7] accomplishes the attack by solving the optimization problem:  $x^A := \min_{x'} \|x' - x\|_2^2 + c \cdot f(x', y)$ , where  $c$  is a constant to balance the perturbation scale and attack success rate, and  $f$  is the adversarial attack loss designed to satisfy the sufficient and necessary condition of different attacks. For instance, the untargeted attack loss is represented as  $f(x', y) = \max(\mathcal{F}(x)_y - \mathcal{F}(x)_{i \neq y}, -\kappa)$  while  $\kappa$  is a confidence variable with value 0.1 as default.

Table 3: Convergence of PGD attack on different ensembles.

Settings		iters	ADP	GAL	DVERGE	TRS
MNIST	$\epsilon = 0.10$	50	4.5	4.1	69.2	<b>93.0</b>
		500	1.6	1.1	66.5	<b>92.8</b>
		1000	1.6	1.0	66.3	<b>92.6</b>
	$\epsilon = 0.15$	50	1.0	0.6	28.8	<b>85.1</b>
		500	0.5	0.1	25.0	<b>83.6</b>
		1000	0.4	0.1	24.8	<b>83.5</b>
CIFAR-10	$\epsilon = 0.01$	50	9.0	8.3	37.1	<b>47.3</b>
		500	3.5	7.8	35.8	<b>47.3</b>
		1000	2.9	7.8	35.7	<b>47.3</b>
	$\epsilon = 0.02$	50	0.1	0.6	10.5	<b>15.5</b>
		500	0.0	0.3	9.0	<b>14.7</b>
		1000	0.0	0.3	8.8	<b>14.7</b>

- *Elastic-net Attack* (EAD) [10] follows the similar optimization of CW Attack while considering both  $\ell_2$  and  $\ell_1$  distortion:  $x^A := \min_{x'} \|x' - x\|_2^2 + \beta \|x' - x\|_1 + c \cdot f(x', y)$ . Here  $\beta, c$  refer to the balancing parameters and  $f(x', y) = \max(\mathcal{F}(x)_y - \mathcal{F}(x)_{i \neq y}, -\kappa)$  under untargeted attack setting. We set  $\beta = 0.01, \kappa = 0.1$  as default.

In our experiments, we set 50 attack iterations with step size  $\alpha = \epsilon/5$  for BIM, MIM attack and PGD attack with 5 random starts. We also verify PGD attack’s convergence by configuring 500 and 1000 iterations. For CW and EAD attacks, we set the number of attack iterations as 1000 and evaluate them with different constant  $c$  for each dataset. We use *Robust Accuracy* as our **evaluation metric** for the whitebox setting, defined as the ratio between the number correctly predicted *adversarial examples* generated by different attacks over the whole test dataset.

**Blackbox robustness evaluation.** Under the blackbox attack setting, we assume the attacker has no knowledge about the target ensemble model, including the model architecture and parameters. In this case, the attacker is only able to craft adversarial examples based on several surrogate models and transfer them to the target victim ensemble model. We follow the same blackbox transfer attack setting as mentioned in [57]: We choose three *Vanilla ensembles* consisting of 3, 5, 8 base models, which are trained with standard Ensemble Cross-Entropy (ECE) loss, as our surrogate models. We apply 50-steps PGD attack with three random starts and two different loss functions (CrossEntropy and CW loss) on each surrogate model to generate adversarial attacks (i.e. for each instance we will have 18 attack attempts). For each instance, among these attack attempts, as long as there is one that can successfully attack the victim model, we will count it as a successful attack. In this case, we report the *Robust Accuracy*, defined as the number of unsuccessful attack attempts divided by the number of all attack attempts, as our **evaluation metric** for the blackbox setting.

## 6.2 Experimental Results

In this section, we present both whitebox and blackbox robustness evaluation results for different ensembles, and show the superiority of the proposed TRS ensemble training. Moreover, we examine the adversarial transferability among base models within different ensembles, which emphasises the effectiveness of the training approaches which aim to increase the base model diversity. We also visualize the decision boundary of different ensembles and discuss the relation to the robustness against different attacks in-depth.

**Whitebox robustness.** Table 1 and 2 present the *Robust Accuracy* of different ensembles against a range of whitebox attacks on MNIST and CIFAR-10 dataset, while CIFAR-100 results are in Appendix G. It is shown that our proposed TRS ensemble outperforms other baseline works including the state-of-the-art DVERGE approach under almost all settings significantly, against a range of attacks and perturbation budgets. Especially, we notice that the performance gap could be larger under stronger adversary attacks (e.g. PGD attack);

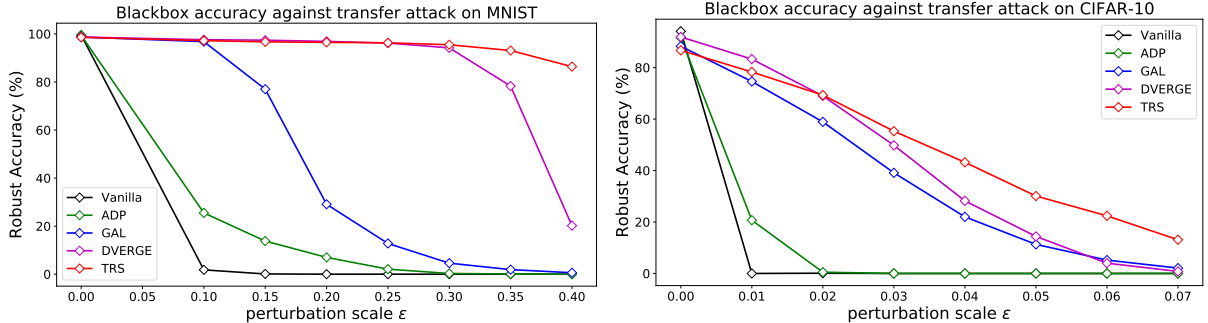


Figure 3: (Top): MNIST; (Bottom): CIFAR-10: Blackbox robust accuracy curve along with different  $\ell_\infty$  perturbation scales  $\epsilon$ .

while TRS ensemble is a bit less robust than baseline methods under FGSM which is a very weak attack. We investigate into this phenomenon in the discussion of model’s decision boundary part.

We observe that when the number of attack iterations is large both ADP and GAL regularizer trained ensemble achieve much lower robust accuracy against iterative attacks (BIM, PGD, MIM) than the reported robustness in the original paper, which is estimated under a small number of attack iterations. This case implies the non-convergence of iterative attack evaluation mentioned in their paper, which is also confirmed by [53]. In the contrast, both DVERGE and TRS still remain highly robust against iterative attacks with large iterations. To show the stability of our model’s robust accuracy, we evaluate it against PGD attack with 500 and 1000 attack iterations. Results are shown in Table 3 where TRS ensemble’s robust accuracy only dropped a little bit after increasing the attack iterations, and outperforms DVERGE by a large margin.

**Blackbox robustness.** Figure 3 shows the *Robust Accuracy* performance of TRS and different baseline ensembles including *Vanilla ensemble*, ADP, GAL, and CVERGE, against blackbox transfer attacks under different perturbation bound  $\epsilon$ . As we can see, the TRS ensemble achieves competitive robust accuracy with DVERGE when  $\epsilon$  is very small, and TRS beats all the baseline works when  $\epsilon$  is large. Precisely speaking, TRS ensemble achieves over 85% robust accuracy against transfer attack with  $\epsilon = 0.4$  on MNIST while the second-best ensemble (DVERGE) only achieves 20.2%. Also for CIFAR-10, TRS ensemble achieves over 25% robust accuracy against transfer attack when  $\epsilon = 0.06$ , while all the other baseline ensembles’ robust accuracy are lower than 6%. This implies that our proposed TRS ensemble has strong generalization ability w.r.t robustness against large  $\epsilon$  adversarial attack than other ensembles by enforcing both small gradient similarity and model smoothness at the same time. We put the numerical blackbox robust accuracy evaluation results in the Appendix E.

**Adversarial transferability.** Figure 4 shows the adversarial transferability matrix of different ensembles against 50-steps PGD attack with  $\epsilon = 0.3$  for MNIST and  $\epsilon = 0.04$  for CIFAR-10. Cell  $(i, j)$ ,  $i \neq j$  represent the transfer attack success rate evaluated on  $j$ -th base model by using the  $i$ -th base model as the surrogate model. Lower number in each cell indicates that the corresponding model is more robust. The diagonal cells, say,  $(i, i)$  refers to  $i$ -th base model’s attack success rate, which reflects the vulnerability of a single model. From these figures, we can see while base models show their vulnerabilities against adversarial attack, only DVERGE and TRS ensemble could achieve low adversarial transferability among base models by adapting effective diverse training. We should also notice that though GAL applied the similar gradient cosine similarity term to our similarity loss  $\mathcal{L}_{\text{sim}}$ , it still can not achieve low adversarial transferability due to the lack of model smoothness enforcement.

**TRS with adversarial training.** While the TRS regularizer could reduce adversarial transferability among base models by enforcing low similarity on loss gradients and promoting model smoothness, we explore whether Adversarial Training [38], which aims to reduce base models’ vulnerability, is able to further improve

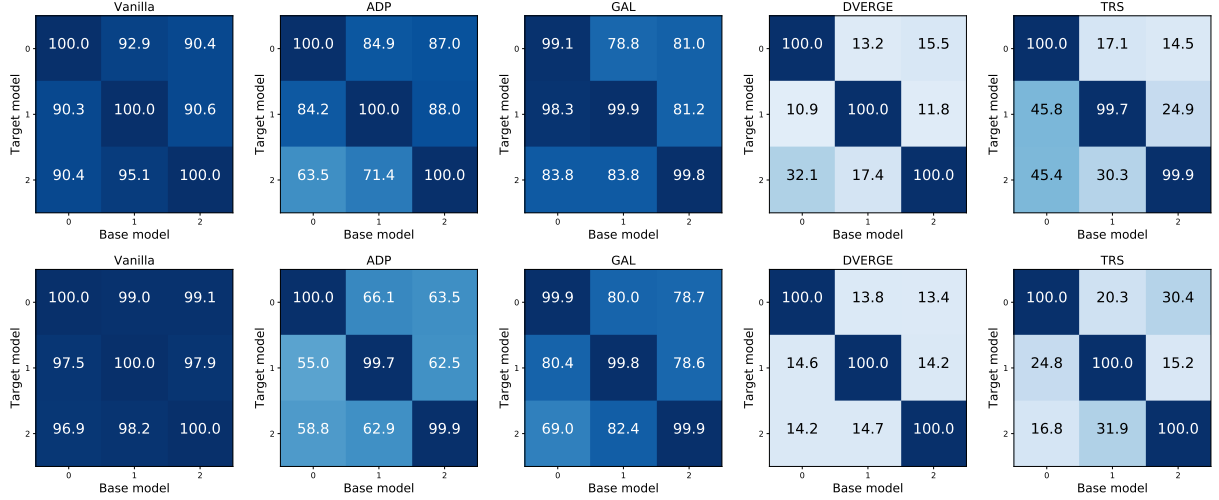


Figure 4: Transferability analysis of the PGD attack on MNIST (top) and CIFAR-10 (bottom). Each cell  $(i, j)$  shows the *attack success rate* of  $i$ -th model on the adversarial examples generated against the  $j$ -th model. We use  $\epsilon = 0.3$  for MNIST and  $\epsilon = 0.04$  for CIFAR-10.

the robustness of TRS or not. We first apply adversarial training to train an ensemble model (AdvT) containing 3 base models as in TRS ensemble. During training, we use  $\ell_\infty$  adversarial perturbation  $\delta_{\text{adv}}$  ( $\|\delta_{\text{adv}}\|_\infty \leq 0.2$  for MNIST and  $\|\delta_{\text{adv}}\|_\infty \leq 0.03$  for CIFAR-10). To combine TRS with adversarial training (TRS+AdvT), we combine TRS regularizer Loss  $\mathcal{L}_{\text{TRS}}$  with Adversarial Training Loss  $\mathcal{L}_{\text{AdvT}} = \max_{\|x-x'\|_\infty \leq \delta_{\text{adv}}} \ell_{\mathcal{F}}(x', y)$  on input  $x$  with label  $y$  with the same weight, and train the ensemble  $\mathcal{F}$  jointly. We evaluate both whitebox and blackbox robustness of TRS+AdvT and AdvT ensembles. During the evaluation, we consider the *Conditional Robust Accuracy* evaluated on adversarial examples generated based on correctly classified clean samples to eliminate the influence of model benign accuracy. For other settings, we follow the same as we discuss in Section 6.1.

Table 4 shows the robustness of both AdvT and TRS+AdvT under whitebox and blackbox attacks on different datasets. As we can see, TRS+AdvT ensemble outperforms the traditional adversarial training based ensemble consistently especially when  $\epsilon$  is large.

### 6.3 Ablation Studies

In this section we visualize the decision boundary of the trained ensembles to gain more insights about the model properties, together with the exploration on the impacts of different loss terms in TRS.

#### Decision boundary analysis.

We visualize the decision boundary of the GAL, DVERGE and TRS ensembles for MNIST and CIFAR-10 in Figure 5. The dashed line is the negative gradient direction and the horizontal direction is randomly chosen which is orthogonal to the gradient direction. From the decision boundary of GAL ensemble, we can see that controlling only the gradient similarity will lead to a very non-smooth model decision boundary and thus harm the model robustness.

From the comparison of DVERGE and TRS ensemble, we find that DVERGE ensemble tends to be more robust along the gradient direction especially on CIFAR-10, (i.e. the distance to the boundary is larger and sometimes even larger than along the other random direction). This may be due to the reason that DVERGE is essentially performing adversarial training for different base models and therefore it protects the adversarial (gradient)

Table 4: Conditional Robust Accuracy (%) of Adversarial Training based ensemble (AdvT) and TRS+AdvT ensemble against (Top) **whitebox attacks** and (Down) **blackbox attack** with different perturbation scales  $\epsilon$ .

Attacks		FGSM		BIM (50)		PGD (50)		MIM (50)	
MNIST	$\epsilon$	0.10	0.20	0.10	0.15	0.10	0.15	0.10	0.15
	AdvT	98.4	97.3	98.2	97.5	98.2	97.2	98.2	97.6
	TRS+AdvT	<b>99.1</b>	<b>98.0</b>	<b>99.0</b>	<b>98.2</b>	<b>98.9</b>	<b>98.0</b>	<b>99.0</b>	<b>98.1</b>
CIFAR-10	$\epsilon$	0.02	0.04	0.01	0.02	0.01	0.02	0.01	0.02
	AdvT	<b>79.3</b>	<b>60.0</b>	88.5	76.1	88.4	76.1	88.5	76.3
	TRS+AdvT	79.2	58.0	<b>90.7</b>	<b>76.7</b>	<b>90.7</b>	<b>76.6</b>	<b>90.9</b>	<b>76.9</b>

MNIST	$\epsilon$	0.10	0.15	0.20	0.25	0.30	0.35	0.40
	AdvT	98.9	98.7	98.6	98.4	98.4	91.6	8.1
	TRS+AdvT	<b>99.4</b>	<b>99.3</b>	<b>99.1</b>	<b>99.1</b>	<b>98.9</b>	<b>98.7</b>	<b>98.5</b>
CIFAR-10	$\epsilon$	0.01	0.02	0.03	0.04	0.05	0.06	0.07
	AdvT	98.4	96.2	93.9	91.5	89.0	84.9	81.1
	TRS+AdvT	<b>98.8</b>	<b>97.7</b>	<b>94.9</b>	<b>92.6</b>	<b>89.9</b>	<b>86.3</b>	<b>81.6</b>

direction. Thus, DVERGE performs better against weak attacks which only consider the gradient direction (e.g. FGSM on CIFAR-10). On the other hand, we find that TRS training yields a smoother model along different directions than DVERGE, which leads to more consistent predictions within a large neighborhood of an input. Thus, the TRS ensemble has higher robustness in different directions against strong attacks such as PGD attack.

**Regularize the similarity loss only.** We consider the case where we only apply our *similarity loss*  $\mathcal{L}_{\text{sim}}$  without *model smoothness loss*  $\mathcal{L}_{\text{smooth}}$  within the TRS (i.e.  $\lambda_b = 0$ ). The result is shown as “Cos-only” in Table 1 and 2, and we observe that its whitebox robustness is much worse than standard TRS. This matches our intuition and theoretical results that only minimizing the gradient similarity cannot guarantee low adversarial transferability among base models and thus lead to low ensemble robustness.

**Comparison between Cos- $\ell_2$  and TRS.** To emphasize the importance of the local min-max training on the model smoothness loss, we train another version of TRS ensemble Cos- $\ell_2$  where we directly apply the  $\ell_2$  regularization on  $\|\nabla_x \ell_{\mathcal{F}}\|_2$  and  $\|\nabla_x \ell_{\mathcal{G}}\|_2$ . The results are shown in the “Cos- $\ell_2$ ” column of Table 1 and 2.

We observe that this simplified TRS ensemble achieves lower robustness accuracy compared with TRS, which implies the necessity of regularizing the gradient magnitude not only on local training points but also on their neighbourhood to ensure overall model smoothness.

## 7 Conclusion

In this paper we aim to deliver an in-depth understanding of adversarial transferability. In doing so, we provide both lower and upper bounds on transferability between low risk classifiers based on gradient

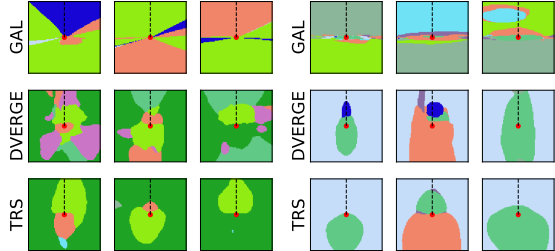


Figure 5: The decision boundary of different models around testing images on (left) MNIST and (right) CIFAR-10 dataset. Same color indicates the same model prediction. The dash lines shows the negative gradient direction, which is used in the gradient-based attacks.

orthogonality and smoothness. We demonstrate theoretically, that smoother models experience tighter lower and upper bounds. We prove that smooth models with lower loss gradient similarity would have lower transferability. Inspired by our analysis, we empirically demonstrate that it is possible to reduce transferability by promoting model smoothness and reducing loss gradient similarity, yielding significant improvement on ensemble robustness.

## References

- [1] Anish Athalye, Nicholas Carlini, and David Wagner. 2018. Obfuscated gradients give a false sense of security: Circumventing defenses to adversarial examples. *arXiv preprint arXiv:1802.00420* (2018).
- [2] Marco Barreno, Blaine Nelson, Anthony D Joseph, and JD Tygar. 2010. The security of machine learning. *Machine Learning* 81, 2 (2010), 121–148.
- [3] Battista Biggio, Igino Corona, Davide Maiorca, Blaine Nelson, Nedim Šrndić, Pavel Laskov, Giorgio Giacinto, and Fabio Roli. 2013. Evasion attacks against machine learning at test time. In *Joint European Conference on Machine Learning and Knowledge Discovery in Databases*. Springer, 387–402.
- [4] Jonathan Borwein and Adrian S Lewis. 2010. *Convex analysis and nonlinear optimization: theory and examples*. Springer Science & Business Media.
- [5] Stephen Boyd and Lieven Vandenberghe. 2004. *Convex Optimization*. Cambridge University Press.
- [6] Wieland Brendel, Jonas Rauber, and Matthias Bethge. 2017. Decision-based adversarial attacks: Reliable attacks against black-box machine learning models. *arXiv preprint arXiv:1712.04248* (2017).
- [7] Nicholas Carlini and David Wagner. 2017. Towards evaluating the robustness of neural networks. In *2017 IEEE Symposium on Security and Privacy (SP)*. IEEE, 39–57.
- [8] Nicholas Carlini and David Wagner. 2017. Towards Evaluating the Robustness of Neural Networks. In *IEEE Symposium on Security and Privacy, 2017*.
- [9] Antonin Chambolle. 2004. An algorithm for total variation minimization and applications. *Journal of Mathematical imaging and vision* 20, 1 (2004), 89–97.
- [10] Pin-Yu Chen, Yash Sharma, Huan Zhang, Jinfeng Yi, and Cho-Jui Hsieh. 2018. Ead: elastic-net attacks to deep neural networks via adversarial examples. In *Thirty-second AAAI conference on artificial intelligence*.
- [11] Sunoh Choi, Jangseong Bae, Changki Lee, Youngsoo Kim, and Jonghyun Kim. 2020. Attention-Based Automated Feature Extraction for Malware Analysis. *Sensors* 20, 10 (2020), 2893.
- [12] Jeremy M Cohen, Elan Rosenfeld, and J Zico Kolter. 2019. Certified adversarial robustness via randomized smoothing. *arXiv preprint arXiv:1902.02918* (2019).
- [13] Francesco Croce and Matthias Hein. 2020. Reliable evaluation of adversarial robustness with an ensemble of diverse parameter-free attacks. *arXiv preprint arXiv:2003.01690* (2020).
- [14] Ambra Demontis, Marco Melis, Maura Pintor, Matthew Jagielski, Battista Biggio, Alina Oprea, Cristina Nita-Rotaru, and Fabio Roli. 2019. Why do adversarial attacks transfer? explaining transferability of evasion and poisoning attacks. In *28th {USENIX} Security Symposium ({USENIX} Security 19)*. 321–338.
- [15] Yinpeng Dong, Fangzhou Liao, Tianyu Pang, Hang Su, Jun Zhu, Xiaolin Hu, and Jianguo Li. 2018. Boosting adversarial attacks with momentum. In *Proceedings of the IEEE conference on computer vision and pattern recognition*. 9185–9193.

[16] Harris Drucker and Yann Le Cun. 1992. Improving generalization performance using double backpropagation. *IEEE Transactions on Neural Networks* 3, 6 (1992), 991–997.

[17] Kevin Eykholt, Ivan Evtimov, Earlence Fernandes, Bo Li, Amir Rahmati, Chaowei Xiao, Atul Prakash, Tadayoshi Kohno, and Dawn Song. 2018. Robust physical-world attacks on deep learning visual classification. In *Proceedings of the IEEE Conference on Computer Vision and Pattern Recognition*. 1625–1634.

[18] Alhussein Fawzi, Omar Fawzi, and Pascal Frossard. 2015. Analysis of classifiers’ robustness to adversarial perturbations. *arXiv preprint arXiv:1502.02590* (2015).

[19] Jerome H Friedman. 2001. Greedy function approximation: a gradient boosting machine. *Annals of statistics* (2001), 1189–1232.

[20] Ian J Goodfellow, Jonathon Shlens, and Christian Szegedy. 2014. Explaining and harnessing adversarial examples. *arXiv preprint arXiv:1412.6572* (2014).

[21] Awni Hannun, Carl Case, Jared Casper, Bryan Catanzaro, Greg Diamos, Erich Elsen, Ryan Prenger, Sanjeev Satheesh, Shubho Sengupta, Adam Coates, et al. 2014. Deep speech: Scaling up end-to-end speech recognition. *arXiv preprint arXiv:1412.5567* (2014).

[22] Trevor Hastie, Saharon Rosset, Ji Zhu, and Hui Zou. 2009. Multi-class adaboost. *Statistics and its Interface* 2, 3 (2009), 349–360.

[23] Kaiming He, Xiangyu Zhang, Shaoqing Ren, and Jian Sun. 2016. Deep residual learning for image recognition. In *Proceedings of the IEEE conference on computer vision and pattern recognition*. 770–778.

[24] Andrew Ilyas, Shibani Santurkar, Dimitris Tsipras, Logan Engstrom, Brandon Tran, and Aleksander Madry. 2019. Adversarial examples are not bugs, they are features. In *Advances in Neural Information Processing Systems*. 125–136.

[25] Sanjay Kariyappa and Moinuddin K Qureshi. 2019. Improving adversarial robustness of ensembles with diversity training. *arXiv preprint arXiv:1901.09981* (2019).

[26] Diederik Kingma and Jimmy Ba. 2014. Adam: A method for stochastic optimization. *arXiv preprint arXiv:1412.6980* (2014).

[27] J Zico Kolter and Eric Wong. 2017. Provable defenses against adversarial examples via the convex outer adversarial polytope. *arXiv preprint arXiv:1711.00851* (2017).

[28] Simon Kornblith, Mohammad Norouzi, Honglak Lee, and Geoffrey Hinton. 2019. Similarity of neural network representations revisited. *arXiv preprint arXiv:1905.00414* (2019).

[29] Alex Krizhevsky, Geoffrey Hinton, et al. 2009. *Learning multiple layers of features from tiny images*. Citeseer.

[30] Alex Krizhevsky, Ilya Sutskever, and Geoffrey E Hinton. 2012. ImageNet classification with deep convolutional neural networks. In *Advances in neural information processing systems*. 1097–1105.

[31] Alexey Kurakin, Ian Goodfellow, and Samy Bengio. 2016. Adversarial examples in the physical world. *arXiv preprint arXiv:1607.02533* (2016).

[32] Yann LeCun. 1998. The MNIST database of handwritten digits. <http://yann.lecun.com/exdb/mnist/> (1998).

[33] Bo Li and Yevgeniy Vorobeychik. 2014. Feature cross-substitution in adversarial classification. In *Advances in Neural Information Processing Systems*. 2087–2095.

[34] Bo Li and Yevgeniy Vorobeychik. 2015. Scalable Optimization of Randomized Operational Decisions in Adversarial Classification Settings.. In *AISTATS*.

[35] Linyi Li, Xiangyu Qi, Tao Xie, and Bo Li. 2020. SoK: Certified Robustness for Deep Neural Networks. *arXiv preprint arXiv:2009.04131* (2020).

[36] Yen-Chen Lin, Zhang-Wei Hong, Yuan-Hong Liao, Meng-Li Shih, Ming-Yu Liu, and Min Sun. 2017. Tactics of Adversarial Attack on Deep Reinforcement Learning Agents. *arXiv preprint arXiv:1703.06748* (2017).

[37] Yanpei Liu, Xinyun Chen, Chang Liu, and Dawn Song. 2016. Delving into transferable adversarial examples and black-box attacks. *arXiv preprint arXiv:1611.02770* (2016).

[38] Aleksander Madry, Aleksandar Makelov, Ludwig Schmidt, Dimitris Tsipras, and Adrian Vladu. 2017. Towards deep learning models resistant to adversarial attacks. *arXiv preprint arXiv:1706.06083* (2017).

[39] Llew Mason, Jonathan Baxter, Peter Bartlett, and Marcus Frean. 1999. Boosting algorithms as gradient descent. *Advances in neural information processing systems* 12 (1999), 512–518.

[40] Seyed-Mohsen Moosavi-Dezfooli, Alhussein Fawzi, Omar Fawzi, and Pascal Frossard. 2016. Universal adversarial perturbations. *arXiv preprint arXiv:1610.08401* (2016).

[41] Adam M Oberman and Jeff Calder. 2018. Lipschitz regularized deep neural networks converge and generalize. *arXiv preprint arXiv:1808.09540* (2018).

[42] Tianyu Pang, Kun Xu, Chao Du, Ning Chen, and Jun Zhu. 2019. Improving adversarial robustness via promoting ensemble diversity. *arXiv preprint arXiv:1901.08846* (2019).

[43] Nicolas Papernot, Patrick McDaniel, and Ian Goodfellow. 2016. Transferability in Machine Learning: from Phenomena to Black-Box Attacks using Adversarial Samples. *arXiv preprint arXiv:1605.07277* (2016).

[44] Nicolas Papernot, Patrick McDaniel, Ian Goodfellow, Somesh Jha, Z Berkay Celik, and Ananthram Swami. 2017. Practical Black-Box Attacks against Deep Learning Systems using Adversarial Examples. In *Proceedings of the 2017 ACM Asia Conference on Computer and Communications Security*.

[45] Nicolas Papernot, Patrick McDaniel, Ian Goodfellow, Somesh Jha, Z Berkay Celik, and Ananthram Swami. 2017. Practical Black-Box Attacks against Machine Learning. In *Proceedings of the 2017 ACM on Asia Conference on Computer and Communications Security*. ACM, 506–519.

[46] Nicolas Papernot, Patrick McDaniel, Somesh Jha, Matt Fredrikson, Z Berkay Celik, and Ananthram Swami. 2016. The limitations of deep learning in adversarial settings. In *2016 IEEE European Symposium on Security and Privacy (EuroS&P)*. IEEE, 372–387.

[47] Pouya Samangouei, Maya Kabkab, and Rama Chellappa. 2018. Defense-GAN: Protecting Classifiers Against Adversarial Attacks Using Generative Models. In *International Conference on Learning Representations*.

[48] Robert E Schapire. 1990. The strength of weak learnability. *Machine learning* 5, 2 (1990), 197–227.

[49] Sahil Singla and Soheil Feizi. 2020. Second-Order Provable Defenses against Adversarial Attacks. In *International Conference on Machine Learning*.

[50] Chawin Sitawarin, Arjun Nitin Bhagoji, Arsalan Mosenia, Mung Chiang, and Prateek Mittal. 2018. DARTS: Deceiving autonomous cars with toxic signs. *arXiv preprint arXiv:1802.06430* (2018).

[51] Ilya Sutskever, Oriol Vinyals, and Quoc V Le. 2014. Sequence to sequence learning with neural networks. In *Advances in neural information processing systems*. 3104–3112.

- [52] Christian Szegedy, Wojciech Zaremba, Ilya Sutskever, Joan Bruna, Dumitru Erhan, Ian Goodfellow, and Rob Fergus. 2014. Intriguing properties of neural networks. In *International Conference on Learning Representations*.
- [53] Florian Tramer, Nicholas Carlini, Wieland Brendel, and Aleksander Madry. 2020. On adaptive attacks to adversarial example defenses. *arXiv preprint arXiv:2002.08347* (2020).
- [54] Florian Tramèr, Nicolas Papernot, Ian Goodfellow, Dan Boneh, and Patrick McDaniel. 2017. The Space of Transferable Adversarial Examples. *arXiv preprint arXiv:1704.03453* (2017).
- [55] Chaowei Xiao, Bo Li, Jun-Yan Zhu, Warren He, Mingyan Liu, and Dawn Song. 2018. Generating adversarial examples with adversarial networks. *arXiv preprint arXiv:1801.02610* (2018).
- [56] Chaowei Xiao, Jun-Yan Zhu, Bo Li, Warren He, Mingyan Liu, and Dawn Song. 2018. Spatially transformed adversarial examples. *arXiv preprint arXiv:1801.02612* (2018).
- [57] Huanrui Yang, Jingyang Zhang, Hongliang Dong, Nathan Inkawich, Andrew Gardner, Andrew Touchet, Wesley Wilkes, Heath Berry, and Hai Li. 2020. DVERGE: Diversifying Vulnerabilities for Enhanced Robust Generation of Ensembles. *Advances in Neural Information Processing Systems* 33 (2020).

## A Discussion: Beyond $\ell_p$ Attack

Besides the widely used  $\ell_p$  norm based adversarial examples, here we plan to extend our understanding to the distribution distance analysis.

We no longer distinguish the targeted attack and untargeted attack. Therefore, we denote either of them by  $\mathcal{A}$ . Moreover, we use  $\mathcal{P}_{\mathcal{A}(x)}$  to represent the distribution of  $\mathcal{A}(x) \in \mathcal{X}$  where  $x$  is distributed according to  $\mathcal{P}_{\mathcal{X}}$ .

Now we define the distribution distance that we use to measure the adversarial distribution gap.

**Definition 8** (Total variation distance; [9]). *For two probability distributions  $\mathcal{P}_{\mathcal{X}}$  and  $\mathcal{P}_{\mathcal{A}(x)}$  on  $\mathcal{X}$ , the total variation distance between them is defined as*

$$\|\mathcal{P}_{\mathcal{X}} - \mathcal{P}_{\mathcal{A}(x)}\|_{TV} = \sup_{C \subseteq \mathcal{X}} |\mathcal{P}_{\mathcal{X}}(C) - \mathcal{P}_{\mathcal{A}(x)}(C)|.$$

Informally, the total variation distance measures the largest change in probability over all events. For discrete probability distributions, the total variation distance is just the  $\ell_1$  distance between the vectors in the probability simplex representing the two distributions.

**Definition 9.** *Given  $\rho \in (0, 1)$ , an attack strategy  $\mathcal{A}(\cdot)$  is called  $\rho$ -conservative, if for  $x \sim \mathcal{P}_{\mathcal{X}}$ ,  $\|\mathcal{P}_{\mathcal{X}} - \mathcal{P}_{\mathcal{A}(x)}\|_{TV} \leq \rho$ .*

This definition formalizes the general objective of generating adversarial examples against deep neural networks: attack samples are likely to be observed, while they do not themselves arouse suspicion.

**Lemma 5.** *Let  $f, g : \mathcal{X} \rightarrow \mathcal{Y}$  be classifiers,  $\delta, \rho, \epsilon \in (0, 1)$  be constants, and  $\mathcal{A}(\cdot)$  be an attack strategy. Suppose that  $\mathcal{A}(\cdot)$  is  $\rho$ -conservative and  $f, g$  have risk at most  $\epsilon$ . Then*

$$\Pr(\mathcal{F}(\mathcal{A}(x)) \neq \mathcal{G}(\mathcal{A}(x))) \leq 2\epsilon + \rho$$

for a given random instance  $x \sim \mathcal{P}_{\mathcal{X}}$ .

*Remark.* This result provides theoretical backing for the intuition that the boundaries of low risk classifiers under certain dense data distribution are close [54]. It considers two classifiers that have risk at most  $\epsilon$ , which indicates their boundaries are close for benign data. It then shows that their boundaries are also close for the perturbed data as long as the attack strategy satisfies a conservative condition which constrains the drift in distribution between the benign and adversarial data.

*Proof of Lemma 5.* Given  $\mathcal{A}(\cdot)$  is  $\rho$ -covert, by Definition 9 we know

$$|\Pr_{\mathcal{P}_{\mathcal{X}}}(f(\mathcal{A}(x)) = g(\mathcal{A}(x))) - \Pr_{\mathcal{X}}(f(x) = g(x))| = |\Pr_{\mathcal{A}(x)}(f(x) = g(x)) - \Pr_{\mathcal{X}}(f(x) = g(x))| \leq \rho.$$

Therefore, we have

$$\Pr(f(\mathcal{A}(x)) = g(\mathcal{A}(x))) \geq \Pr(f(x) = g(x)) - \rho.$$

From the low-risk conditions, the classifiers agree w.h.p.

$$\begin{aligned} & \Pr(f(\mathcal{A}(x)) \neq g(\mathcal{A}(x))) \\ & \leq \Pr(f(x) \neq g(x)) + \rho \\ & \leq 1 - \Pr(f(x) = y, g(x) = y) + \rho, \quad ^1 \\ & \leq 1 - (1 - \Pr(f(x) \neq y) - \Pr(g(x) \neq y)) + \rho \\ & = \epsilon + \epsilon + \rho \\ & \leq 2\epsilon + \rho, \end{aligned}$$

where the third inequality follows from the union bound. <sup>2</sup> □

<sup>1</sup>Here we assume  $y$  is the ground truth label.

<sup>2</sup>Recall that for arbitrary events  $A_1, \dots, A_n$ , the union bound implies  $P(\bigcap_{i=1}^n A_i) \geq 1 - \sum_{i=1}^n P(\overline{A_i})$ .

**Theorem 6.** Let  $\mathcal{F}, \mathcal{G} : \mathcal{X} \rightarrow \mathcal{Y}$  be classifiers ( $\mathcal{Y} \in \{-1, 1\}$ ),  $\delta, \rho, \epsilon \in (0, 1)$  be constants, and  $\mathcal{A}(\cdot)$  an attack strategy. Suppose that  $\mathcal{A}(\cdot)$  is  $\rho$ -conservative and  $\mathcal{F}, \mathcal{G}$  have risk at most  $\epsilon$ . Given random instance  $x \in \mathcal{X}$ , if  $\mathcal{A}(\cdot)$  is  $(\delta, \mathcal{F})$ -effective, then it is also  $(\delta + 4\epsilon + \rho, \mathcal{G})$ -effective.

*Proof.* From Lemma 5, and the union bound we have

$$\begin{aligned} & \Pr(f(x) \neq f(\mathcal{A}(x))) \\ & \geq \Pr(g(x) \neq g(\mathcal{A}(x)), f(x) = g(x), f(\mathcal{A}(x)) = g(\mathcal{A}(x))) \\ & \geq 1 - \Pr(g(x) = g(\mathcal{A}(x))) - \Pr(f(x) \neq g(x)) - \Pr(f(\mathcal{A}(x)) \neq g(\mathcal{A}(x))) \\ & \geq 1 - \delta - 4\epsilon - \rho, \end{aligned}$$

as claimed.  $\square$

The proof is shown below. This result formalizes the intuition that low-risk classifiers possess close decision boundaries in high-probability regions. The proof is deferred to Appendix A. In such settings, an attack strategy that successfully attacks one classifier would have high probability to mislead the other. This theorem explains why we should expect successful transferability in practice: defenders will naturally prefer low-risk binary classifiers. This desirable quality of classifiers is a potential liability.

*Proof of Theorem 6.* From Lemma 5, and the union bound we have

$$\begin{aligned} & \Pr(g(x) \neq g(\mathcal{A}(x))) \\ & \geq \Pr(f(x) \neq f(\mathcal{A}(x)), g(x) = f(x), g(\mathcal{A}(x)) = f(\mathcal{A}(x))) \\ & \geq 1 - \Pr(f(x) = f(\mathcal{A}(x))) - \Pr(g(x) \neq f(x)) - \Pr(g(\mathcal{A}(x)) \neq f(\mathcal{A}(x))) \\ & \geq 1 - \delta - 4\epsilon - \rho, \end{aligned}$$

as claimed.  $\square$

## B Proof of Transferability Lower Bound (Theorems 1 and 2)

Here we present the proof of Theorem 1 and Theorem 2 first stated in Section 4.3.

The following lemma is used in the proof.

**Lemma 7.** For arbitrary vector  $\delta$ ,  $x$ ,  $y$ , when  $\|\delta\|_2 \leq \epsilon$ ,  $x$  and  $y$  are unit vectors, i.e.,  $\|x\|_2 = \|y\|_2 = 1$ ,  $\cos\langle x, y \rangle = \frac{x \cdot y}{\|x\|_2 \cdot \|y\|_2} = m$ . Let  $c$  denote any real number. Then

$$\delta \cdot y > c + \epsilon\sqrt{2 - 2m} \Rightarrow \delta \cdot x > c.$$

*Proof.*  $\delta \cdot x = \delta \cdot y + \delta \cdot (x - y) > c + \epsilon\sqrt{2 - 2m} + \delta \cdot (x - y)$ . By law of cosines,  $\delta \cdot (x - y) \geq -\epsilon\sqrt{2 - 2\cos\langle x, y \rangle} = -\epsilon\sqrt{2 - 2m}$ . Hence,  $\delta \cdot x > c$ .  $\square$

**Theorem** (Lower Bound on Targeted Attack Transferability). Assume both models  $\mathcal{F}$  and  $\mathcal{G}$  are  $\beta$ -smooth. Let  $\mathcal{A}_T$  be an  $(\alpha, \mathcal{F})$ -effective targeted attack with perturbation ball  $\|\delta\|_2 \leq \epsilon$  and target label  $y_t \in \mathcal{Y}$ . The transferability can be lower bounded by

$$\Pr(T_r(\mathcal{F}, \mathcal{G}, x, y_t) = 1) \geq (1 - \alpha) - (\eta_{\mathcal{F}} + \eta_{\mathcal{G}}) - \frac{\epsilon(1 + \alpha) + c_{\mathcal{F}}(1 - \alpha)}{c_{\mathcal{G}} + \epsilon} - \frac{\epsilon(1 - \alpha)}{c_{\mathcal{G}} + \epsilon} \sqrt{2 - 2\mathcal{S}(\ell_{\mathcal{F}}, \ell_{\mathcal{G}})},$$

where

$$c_{\mathcal{F}} = \max_{x \in \mathcal{X}} \frac{\min_{y \in \mathcal{Y}} \ell_{\mathcal{F}}(\mathcal{A}_T(x), y) - \ell_{\mathcal{F}}(x, y_t) + \beta\epsilon^2/2}{\|\nabla_x \ell_{\mathcal{F}}(x, y_t)\|_2}, \quad c_{\mathcal{G}} = \min_{x \in \mathcal{X}} \frac{\min_{y \in \mathcal{Y}} \ell_{\mathcal{G}}(\mathcal{A}_T(x), y) - \ell_{\mathcal{G}}(x, y_t) - \beta\epsilon^2/2}{\|\nabla_x \ell_{\mathcal{G}}(x, y_t)\|_2}.$$

Here  $\eta_{\mathcal{F}}, \eta_{\mathcal{G}}$  are the risks of models  $\mathcal{F}$  and  $\mathcal{G}$  respectively.

*Proof.* For simplifying the notations, we define  $x^{\mathcal{A}} := \mathcal{A}_T(x)$ , which is the generated adversarial example by  $\mathcal{A}_T$  when the input is  $x$ .

Define auxiliary function  $f, g : \mathcal{X} \mapsto \mathbb{R}$  such that

$$f(x) = \frac{\min_{y \in \mathcal{Y}} \ell_{\mathcal{F}}(x^{\mathcal{A}}, y) - \ell_{\mathcal{F}}(x, y_t) + \beta\epsilon^2/2}{\|\nabla_x \ell_{\mathcal{F}}(x, y_t)\|_2}, \quad g(x) = \frac{\min_{y \in \mathcal{Y}} \ell_{\mathcal{G}}(x^{\mathcal{A}}, y) - \ell_{\mathcal{G}}(x, y_t) - \beta\epsilon^2/2}{\|\nabla_x \ell_{\mathcal{G}}(x, y_t)\|_2}.$$

The  $f$  and  $g$  are orthogonal to the confidence score functions of model  $\mathcal{F}$  and  $\mathcal{G}$ . Note that  $c_{\mathcal{F}} = \max_{x \in \mathcal{X}} f(x)$  and  $c_{\mathcal{G}} = \min_{x \in \mathcal{X}} g(x)$ .

The transferability of concern satisfies:

$$\begin{aligned} & \Pr(T_r(\mathcal{F}, \mathcal{G}, x, y_t) = 1) \\ &= \Pr(\mathcal{F}(x) = y \cap \mathcal{G}(x) = y \cap \mathcal{F}(x^{\mathcal{A}}) = y_t \cap \mathcal{G}(x^{\mathcal{A}}) = y_t) \end{aligned} \tag{1}$$

$$\geq 1 - \Pr(\mathcal{F}(x) \neq y) - \Pr(\mathcal{G}(x) \neq y) - \Pr(\mathcal{F}(x^{\mathcal{A}}) \neq y_t) - \Pr(\mathcal{G}(x^{\mathcal{A}}) \neq y_t) \tag{2}$$

$$\geq 1 - \eta_{\mathcal{F}} - \eta_{\mathcal{G}} - \alpha - \Pr(\mathcal{G}(x^{\mathcal{A}}) \neq y_t). \tag{3}$$

Eq. 1 follows the definition (Definition 7). Eq. 1 to Eq. 2 follows from the union bound. From Eq. 1 to Eq. 2 definition of model risk and definition of adversarial effectiveness (Definition 2) are applied.

Now consider  $\Pr(\mathcal{F}(x^{\mathcal{A}}) \neq y_t)$  and  $\Pr(\mathcal{G}(x^{\mathcal{A}}) \neq y_t)$ . Given that model predicts the label for which  $\ell_{\mathcal{F}}$  is minimized,  $\mathcal{F}(x^{\mathcal{A}}) \neq y_t \iff \ell_{\mathcal{F}}(x + \delta, y_t) > \min_y \ell_{\mathcal{F}}(x + \delta, y)$ . Similarly,  $\mathcal{G}(x^{\mathcal{A}}) \neq y_t \iff \ell_{\mathcal{G}}(x + \delta, y_t) > \min_y \ell_{\mathcal{G}}(x + \delta, y)$ .

Following Taylor's Theorem with Lagrange remainder, we have

$$\ell_{\mathcal{F}}(x + \delta, y_t) = \ell_{\mathcal{F}}(x, y_t) + \delta \nabla_x \ell_{\mathcal{F}}(x, y_t) + \frac{1}{2} \xi^\top \mathbf{H}_{\mathcal{F}} \xi, \quad (4)$$

$$\ell_{\mathcal{G}}(x + \delta, y_t) = \ell_{\mathcal{G}}(x, y_t) + \delta \nabla_x \ell_{\mathcal{G}}(x, y_t) + \frac{1}{2} \xi^\top \mathbf{H}_{\mathcal{G}} \xi. \quad (5)$$

In Eq. 4 and Eq. 5,  $\xi = k\delta$  for some  $k \in [0, 1]$ .  $\mathbf{H}_{\mathcal{F}}$  and  $\mathbf{H}_{\mathcal{G}}$  are Hessian matrices of  $\ell_{\mathcal{F}}$  and  $\ell_{\mathcal{G}}$  respectively. Since  $\ell_{\mathcal{F}}(x + \delta, y_t)$  and  $\ell_{\mathcal{G}}(x + \delta, y_t)$  are  $\beta$ -smooth, the maximum eigenvalues of  $\mathbf{H}_{\mathcal{F}}$  and  $\mathbf{H}_{\mathcal{G}}$  are bounded by  $\beta$ . As the result,  $|\xi^\top \mathbf{H}_{\mathcal{F}} \xi| \leq \beta \cdot \|\xi\|_2^2 \leq \beta \epsilon^2$ . Applying them to Eq. 4 and Eq. 5, we thus have

$$\ell_{\mathcal{F}}(x, y_t) + \delta \nabla_x \ell_{\mathcal{F}}(x, y_t) - \frac{1}{2} \beta \epsilon^2 \leq \ell_{\mathcal{F}}(x + \delta, y_t) \leq \ell_{\mathcal{F}}(x, y_t) + \delta \nabla_x \ell_{\mathcal{F}}(x, y_t) + \frac{1}{2} \beta \epsilon^2, \quad (6)$$

$$\ell_{\mathcal{G}}(x, y_t) + \delta \nabla_x \ell_{\mathcal{G}}(x, y_t) - \frac{1}{2} \beta \epsilon^2 \leq \ell_{\mathcal{G}}(x + \delta, y_t) \leq \ell_{\mathcal{G}}(x, y_t) + \delta \nabla_x \ell_{\mathcal{G}}(x, y_t) + \frac{1}{2} \beta \epsilon^2. \quad (7)$$

Apply left hand side of Eq. 6 to  $\Pr(\mathcal{F}(x^{\mathcal{A}}) \neq y_t) \leq \alpha$  (from Definition 2):

$$\begin{aligned} & \Pr(\mathcal{F}(x^{\mathcal{A}}) \neq y_t) \\ &= \Pr\left(\ell_{\mathcal{F}}(x + \delta, y_t) > \min_y \ell_{\mathcal{F}}(x + \delta, y)\right) \\ &\geq \Pr\left(\ell_{\mathcal{F}}(x, y_t) + \delta \nabla_x \ell_{\mathcal{F}}(x, y_t) - \frac{1}{2} \beta \epsilon^2 > \min_y \ell_{\mathcal{F}}(x + \delta, y)\right) \\ &= \Pr\left(\delta \cdot \frac{\nabla_x \ell_{\mathcal{F}}(x, y_t)}{\|\nabla_x \ell_{\mathcal{F}}(x, y_t)\|_2} > f(x)\right), \\ &\implies \Pr\left(\delta \cdot \frac{\nabla_x \ell_{\mathcal{F}}(x, y_t)}{\|\nabla_x \ell_{\mathcal{F}}(x, y_t)\|_2} > f(x)\right) \leq \alpha. \end{aligned}$$

Similarly, we apply right hand side of Eq. 7 to  $\Pr(\mathcal{G}(x^{\mathcal{A}}) = y_t)$ :

$$\begin{aligned} & \Pr(\mathcal{G}(x^{\mathcal{A}}) \neq y_t) \\ &= \Pr\left(\ell_{\mathcal{G}}(x + \delta, y_t) > \min_y \ell_{\mathcal{G}}(x + \delta, y)\right) \\ &\leq \Pr\left(\ell_{\mathcal{G}}(x, y_t) + \delta \nabla_x \ell_{\mathcal{G}}(x, y_t) + \frac{1}{2} \beta \epsilon^2 > \min_y \ell_{\mathcal{G}}(x + \delta, y)\right) \\ &= \Pr\left(\delta \cdot \frac{\nabla_x \ell_{\mathcal{G}}(x, y_t)}{\|\nabla_x \ell_{\mathcal{G}}(x, y_t)\|_2} > g(x)\right). \end{aligned} \quad (8)$$

Knowing that  $\|\delta\|_2 \leq \epsilon$ , from Lemma 7 we have

$$\delta \cdot \frac{\nabla_x \ell_{\mathcal{G}}(x, y_t)}{\|\nabla_x \ell_{\mathcal{G}}(x, y_t)\|_2} > f(x) + \epsilon \sqrt{2 - 2\underline{\mathcal{S}}(\ell_{\mathcal{F}}, \ell_{\mathcal{G}})} \quad (9)$$

$$\implies \delta \cdot \frac{\nabla_x \ell_{\mathcal{G}}(x, y_t)}{\|\nabla_x \ell_{\mathcal{G}}(x, y_t)\|_2} > f(x) + \epsilon \sqrt{2 - 2 \cos \langle \nabla_x \ell_{\mathcal{F}}(x, y_t), \nabla_x \ell_{\mathcal{G}}(x, y_t) \rangle} \quad (10)$$

$$\implies \delta \cdot \frac{\nabla_x \ell_{\mathcal{F}}(x, y_t)}{\|\nabla_x \ell_{\mathcal{F}}(x, y_t)\|_2} > f(x). \quad (11)$$

From Eq. 9 to Eq. 10, the infimum in definition of  $\underline{\mathcal{S}}$  (Definition 4) indicates that

$$\underline{\mathcal{S}}(\ell_{\mathcal{F}}, \ell_{\mathcal{G}}) \leq \cos \langle \nabla_x \ell_{\mathcal{F}}(x, y_t), \nabla_x \ell_{\mathcal{G}}(x, y_t) \rangle.$$

Hence,

$$f(x) + \epsilon \sqrt{2 - 2\underline{\mathcal{S}}(\ell_{\mathcal{F}}, \ell_{\mathcal{G}})} \geq f(x) + \epsilon \sqrt{2 - 2 \cos \langle \nabla_x \ell_{\mathcal{F}}(x, y_t), \nabla_x \ell_{\mathcal{G}}(x, y_t) \rangle}.$$

Eq. 10 to Eq. 11 directly uses Lemma 7. As the result,

$$\Pr \left( \delta \cdot \frac{\nabla_x \ell_{\mathcal{G}}(x, y_t)}{\|\nabla_x \ell_{\mathcal{G}}(x, y_t)\|_2} > f(x) + \epsilon \sqrt{2 - 2\underline{\mathcal{S}}(\ell_{\mathcal{F}}, \ell_{\mathcal{G}})} \right) \leq \Pr \left( \delta \cdot \frac{\nabla_x \ell_{\mathcal{F}}(x, y_t)}{\|\nabla_x \ell_{\mathcal{F}}(x, y_t)\|_2} > f(x) \right) \leq \alpha.$$

Note that  $f(x) \leq c_{\mathcal{F}}$ , we have

$$\Pr \left( \delta \cdot \frac{\nabla_x \ell_{\mathcal{G}}(x, y_t)}{\|\nabla_x \ell_{\mathcal{G}}(x, y_t)\|_2} > c_{\mathcal{F}} + \epsilon \sqrt{2 - 2\underline{\mathcal{S}}(\ell_{\mathcal{F}}, \ell_{\mathcal{G}})} \right) \leq \alpha.$$

Now we consider the maximum expectation of  $\delta \cdot \frac{\nabla_x \ell_{\mathcal{G}}(x, y_t)}{\|\nabla_x \ell_{\mathcal{G}}(x, y_t)\|_2}$ . Its maximum is  $\max \|\delta\|_2 = \epsilon$ . Therefore, its expectation is bounded:

$$\mathbb{E} \left[ \delta \cdot \frac{\nabla_x \ell_{\mathcal{G}}(x, y_t)}{\|\nabla_x \ell_{\mathcal{G}}(x, y_t)\|_2} \right] \leq \epsilon \cdot \alpha + (c_{\mathcal{F}} + \epsilon \sqrt{2 - 2\underline{\mathcal{S}}(\ell_{\mathcal{F}}, \ell_{\mathcal{G}})}) (1 - \alpha).$$

Now applying Markov's inequality, we get

$$\begin{aligned} & \Pr \left( \delta \cdot \frac{\nabla_x \ell_{\mathcal{G}}(x, y_t)}{\|\nabla_x \ell_{\mathcal{G}}(x, y_t)\|_2} > c_{\mathcal{G}} \right) \\ & \leq \frac{\epsilon \cdot \alpha + (c_{\mathcal{F}} + \epsilon \sqrt{2 - 2\underline{\mathcal{S}}(\ell_{\mathcal{F}}, \ell_{\mathcal{G}})}) (1 - \alpha) + \epsilon}{c_{\mathcal{G}} + \epsilon} \\ & = \frac{\epsilon(1 + \alpha) + (c_{\mathcal{F}} + \epsilon \sqrt{2 - 2\underline{\mathcal{S}}(\ell_{\mathcal{F}}, \ell_{\mathcal{G}})}) (1 - \alpha)}{c_{\mathcal{G}} + \epsilon}. \end{aligned}$$

Since  $g(x) \geq c_{\mathcal{G}}$ ,

$$\Pr \left( \delta \cdot \frac{\nabla_x \ell_{\mathcal{G}}(x, y_t)}{\|\nabla_x \ell_{\mathcal{G}}(x, y_t)\|_2} > g(x) \right) \leq \Pr \left( \delta \cdot \frac{\nabla_x \ell_{\mathcal{G}}(x, y_t)}{\|\nabla_x \ell_{\mathcal{G}}(x, y_t)\|_2} > c_{\mathcal{G}} \right) \leq \frac{\epsilon(1 + \alpha) + (c_{\mathcal{F}} + \epsilon \sqrt{2 - 2\underline{\mathcal{S}}(\ell_{\mathcal{F}}, \ell_{\mathcal{G}})}) (1 - \alpha)}{c_{\mathcal{G}} + \epsilon}.$$

Combine with Eq. 11, finally,

$$\begin{aligned} & \Pr(T_r(\mathcal{F}, \mathcal{G}, x, y_t) = 1) \\ & \geq 1 - \eta_{\mathcal{F}} - \eta_{\mathcal{G}} - \alpha - \Pr(\mathcal{G}(x^{\mathcal{A}}) \neq y_t) \\ & \stackrel{(i.)}{\geq} 1 - \eta_{\mathcal{F}} - \eta_{\mathcal{G}} - \alpha - \Pr \left( \delta \cdot \frac{\nabla_x \ell_{\mathcal{G}}(x, y_t)}{\|\nabla_x \ell_{\mathcal{G}}(x, y_t)\|_2} > g(x) \right) \\ & \geq 1 - \eta_{\mathcal{F}} - \eta_{\mathcal{G}} - \alpha - \frac{\epsilon(1 + \alpha) + (c_{\mathcal{F}} + \epsilon \sqrt{2 - 2\underline{\mathcal{S}}(\ell_{\mathcal{F}}, \ell_{\mathcal{G}})}) (1 - \alpha)}{c_{\mathcal{G}} + \epsilon} \\ & = (1 - \alpha) - (\eta_{\mathcal{F}} + \eta_{\mathcal{G}}) - \frac{\epsilon(1 + \alpha) + c_{\mathcal{F}}(1 - \alpha)}{c_{\mathcal{G}} + \epsilon} - \frac{\epsilon(1 - \alpha)}{c_{\mathcal{G}} + \epsilon} \sqrt{2 - 2\underline{\mathcal{S}}(\ell_{\mathcal{F}}, \ell_{\mathcal{G}})}. \end{aligned}$$

Here, (i.) follows Eq. 8.  $\square$

**Theorem** (Lower Bound on Untargeted Attack Transferability). *Assume both models  $\mathcal{F}$  and  $\mathcal{G}$  are  $\beta$ -smooth. Let  $\mathcal{A}_U$  be an  $(\alpha, \mathcal{F})$ -effective untargeted attack with perturbation ball  $\|\delta\|_2 \leq \epsilon$ . The transferability can be lower bounded by*

$$\Pr(T_r(\mathcal{F}, \mathcal{G}, x) = 1) \geq (1 - \alpha) - (\eta_{\mathcal{F}} + \eta_{\mathcal{G}}) - \frac{\epsilon(1 + \alpha) - c_{\mathcal{F}}(1 - \alpha)}{\epsilon - c_{\mathcal{G}}} - \frac{\epsilon(1 - \alpha)}{\epsilon - c_{\mathcal{G}}} \sqrt{2 - 2\underline{\mathcal{S}}(\ell_{\mathcal{F}}, \ell_{\mathcal{G}})},$$

where

$$c_{\mathcal{F}} = \min_{(x,y) \in \text{supp}(\mathcal{D})} \frac{\min_{y' \in \mathcal{Y}: y' \neq y} \ell_{\mathcal{F}}(\mathcal{A}_U(x), y') - \ell_{\mathcal{F}}(x, y) - \beta\epsilon^2/2}{\|\nabla_x \ell_{\mathcal{F}}(x, y)\|_2}, \quad c_{\mathcal{G}} = \max_{(x,y) \in \text{supp}(\mathcal{D})} \frac{\min_{y' \in \mathcal{Y}: y' \neq y} \ell_{\mathcal{G}}(\mathcal{A}_U(x), y') - \ell_{\mathcal{G}}(x, y) + \beta\epsilon^2/2}{\|\nabla_x \ell_{\mathcal{G}}(x, y)\|_2}.$$

Here  $\eta_{\mathcal{F}}$  and  $\eta_{\mathcal{G}}$  are the risks of models  $\mathcal{F}$  and  $\mathcal{G}$  respectively. The  $\text{supp}(\mathcal{D})$  is the support of benign data distribution, i.e.,  $x$  is the benign data and  $y$  is its associated true label.

*Proof.* For simplifying the notations, we define  $x^{\mathcal{A}} := \mathcal{A}_U(x)$ , which is the generated adversarial example by  $\mathcal{A}_U$  when the input is  $x$ . Define auxiliary function  $f, g : \mathcal{M} \rightarrow \mathbb{R}$  such that

$$f(x, y) = \frac{\min_{y' \in \mathcal{Y}: y' \neq y} \ell_{\mathcal{F}}(x^{\mathcal{A}}, y') - \ell_{\mathcal{F}}(x, y) - \beta\epsilon^2/2}{\|\nabla_x \ell_{\mathcal{F}}(x, y)\|_2}, \quad g(x, y) = \frac{\min_{y' \in \mathcal{Y}: y' \neq y} \ell_{\mathcal{G}}(x^{\mathcal{A}}, y') - \ell_{\mathcal{G}}(x, y) + \beta\epsilon^2/2}{\|\nabla_x \ell_{\mathcal{G}}(x, y)\|_2}.$$

The  $f$  and  $g$  are orthogonal to the confidence score functions of model  $\mathcal{F}$  and  $\mathcal{G}$ . Note that

$$c_{\mathcal{F}} = \min_{(x,y) \in \text{supp}(\mathcal{D})} f(x, y), \quad c_{\mathcal{G}} = \max_{(x,y) \in \text{supp}(\mathcal{D})} g(x, y).$$

The proof is similar to that of Theorem 1.

$$\begin{aligned} & \Pr(T_r(\mathcal{F}, \mathcal{G}, x) = 1) \\ &= \Pr(\mathcal{F}(x) = y \cap \mathcal{G}(x) = y \cap \mathcal{F}(x^{\mathcal{A}}) \neq y \cap \mathcal{G}(x^{\mathcal{A}}) \neq y) \\ &\geq 1 - \Pr(\mathcal{F}(x) \neq y) - \Pr(\mathcal{G}(x) \neq y) - \Pr(\mathcal{F}(x^{\mathcal{A}}) = y) - \Pr(\mathcal{G}(x^{\mathcal{A}}) = y) \\ &= 1 - \eta_{\mathcal{F}} - \eta_{\mathcal{G}} - \alpha - \Pr(\mathcal{G}(x^{\mathcal{A}}) = y). \end{aligned} \tag{12}$$

From Taylor's Theorem and Lemma 7, we observe that

$$\Pr(\mathcal{G}(x^{\mathcal{A}}) = y) \leq \Pr\left(\delta \cdot \frac{\nabla_x \ell_{\mathcal{G}}(x, y)}{\|\nabla_x \ell_{\mathcal{G}}(x, y)\|_2} < c_{\mathcal{G}}\right), \tag{13}$$

$$\Pr\left(\delta \cdot \frac{\nabla_x \ell_{\mathcal{G}}(x, y)}{\|\nabla_x \ell_{\mathcal{G}}(x, y)\|_2} < c_{\mathcal{F}} - \epsilon\sqrt{2 - 2\mathcal{S}(\ell_{\mathcal{F}}, \ell_{\mathcal{G}})}\right) \leq \Pr(\mathcal{F}(x^{\mathcal{A}}) = y) = \alpha. \tag{14}$$

According to Markov's inequality, Eq. 14 implies that

$$\Pr\left(\delta \cdot \frac{\nabla_x \ell_{\mathcal{G}}(x, y)}{\|\nabla_x \ell_{\mathcal{G}}(x, y)\|_2} < c_{\mathcal{G}}\right) \leq \frac{\epsilon(1 + \alpha) - (c_{\mathcal{F}} - \epsilon\sqrt{2 - 2\mathcal{S}(\ell_{\mathcal{F}}, \ell_{\mathcal{G}})})(1 - \alpha)}{\epsilon - c_{\mathcal{G}}}. \tag{15}$$

We conclude the proof by combining Eq. 13 with Eq. 15 and plugging it into Eq. 12.  $\square$

## C Proof of Transferability Upper Bound (Theorems 3 and 4)

Here we present the proof of Theorem 3 and Theorem 4 as stated in Section 4.4.

The following lemma is used in the proof.

**Lemma 8.** Suppose two unit vectors  $x, y$  satisfy  $x \cdot y < S$ , then for any  $\delta$ , we have  $\min(\delta \cdot x, \delta \cdot y) < \|\delta\|_2 \sqrt{(1 + S)/2}$ .

*Proof.* For sake of contradiction, suppose  $\delta \cdot x > \|\delta\|_2 \sqrt{(1 + S)/2}$ ,  $\delta \cdot y > \|\delta\|_2 \sqrt{(1 + S)/2}$ . Denote  $\alpha$  to be the angel between  $x$  and  $y$ , then  $\cos \alpha < S$ , or  $\alpha > \arccos S$ . If  $\alpha_x, \alpha_y$  are the angles between  $\delta$  and  $x$  and between  $\delta$  and  $y$  respectively, then we have  $\max(\alpha_x, \alpha_y) \geq \alpha/2 \geq \arccos S/2$ . Thus  $\min(\delta \cdot x, \delta \cdot y) \leq \|\delta\|_2 \cos(\alpha/2) = \|\delta\|_2 \sqrt{(1 + S)/2}$ .  $\square$

**Theorem** (Upper Bound on Targeted Attack Transferability). *Assume both model  $\mathcal{F}$  and  $\mathcal{G}$  are  $\beta$ -smooth with gradient magnitude bounded by  $B$ , i.e.,  $\|\nabla_x \ell_{\mathcal{F}}(x, y)\| \leq B$  and  $\|\nabla_x \ell_{\mathcal{G}}(x, y)\| \leq B$  for any  $x \in \mathcal{X}, y \in \mathcal{Y}$ . Let  $\mathcal{A}_T$  be an  $(\alpha, \mathcal{F})$ -effective targeted attack with perturbation ball  $\|\delta\|_2 \leq \epsilon$  and target label  $y_t \in \mathcal{Y}$ . The transferability can be upper bounded by*

$$\Pr(T_r(\mathcal{F}, \mathcal{G}, x, y_t) = 1) \leq \frac{\xi_{\mathcal{F}} + \xi_{\mathcal{G}}}{\ell_{\min} - \epsilon B \left(1 + \sqrt{\frac{1 + \bar{\mathcal{S}}(\ell_{\mathcal{F}}, \ell_{\mathcal{G}})}{2}}\right) - \beta \epsilon^2},$$

where

$$\ell_{\min} = \min_{x \in \mathcal{X}} (\ell_{\mathcal{F}}(x, y_t), \ell_{\mathcal{G}}(x, y_t)).$$

Here  $\xi_{\mathcal{F}}$  and  $\xi_{\mathcal{G}}$  are the empirical risks of models  $\mathcal{F}$  and  $\mathcal{G}$  respectively, defined relative to a differentiable loss.

*Proof.* We let  $x^{\mathcal{A}} := \mathcal{A}_T(x)$  be the generated adversarial example when the input is  $x$ . Since  $\mathcal{F}(x)$  outputs label for which  $\ell_{\mathcal{F}}$  is minimized, we have

$$\mathcal{F}(x) = y \implies \ell_{\mathcal{F}}(x, y_t) > \ell_{\mathcal{F}}(x, y) \quad (16)$$

and similarly

$$\mathcal{F}(x^{\mathcal{A}}) = y_t \implies \ell_{\mathcal{F}}(x^{\mathcal{A}}, y) > \ell_{\mathcal{F}}(x^{\mathcal{A}}, y_t), \quad (17)$$

$$\mathcal{G}(x) = y \implies \ell_{\mathcal{G}}(x, y_t) > \ell_{\mathcal{G}}(x, y), \quad (18)$$

$$\mathcal{G}(x^{\mathcal{A}}) = y_t \implies \ell_{\mathcal{G}}(x^{\mathcal{A}}, y) > \ell_{\mathcal{G}}(x^{\mathcal{A}}, y_t). \quad (19)$$

Since  $\ell_{\mathcal{F}}(x, y)$  and  $\ell_{\mathcal{G}}(x, y)$  are  $\beta$ -smooth,

$$\ell_{\mathcal{F}}(x, y) + \delta \cdot \nabla_x \ell_{\mathcal{F}}(x, y) + \frac{\beta}{2} \|\delta\|^2 \geq \ell_{\mathcal{F}}(x^{\mathcal{A}}, y),$$

which implies

$$\begin{aligned} \delta \cdot \nabla_x \ell_{\mathcal{F}}(x, y) &\geq \ell_{\mathcal{F}}(x^{\mathcal{A}}, y) - \ell_{\mathcal{F}}(x, y) - \frac{\beta}{2} \|\delta\|^2 \\ &\geq \ell_{\mathcal{F}}(x^{\mathcal{A}}, y_t) - \ell_{\mathcal{F}}(x, y) - \frac{\beta}{2} \|\delta\|^2 =: c'_{\mathcal{F}}. \end{aligned} \quad (20)$$

Similarly for  $\mathcal{G}$ ,

$$\delta \cdot \nabla_x \ell_{\mathcal{G}}(x, y) \geq \ell_{\mathcal{G}}(x^{\mathcal{A}}, y_t) - \ell_{\mathcal{G}}(x, y) - \frac{\beta}{2} \|\delta\|^2 =: c'_{\mathcal{G}}. \quad (21)$$

Thus,

$$\Pr(\mathcal{F}(x) = y, \mathcal{G}(x) = y, \mathcal{F}(x^{\mathcal{A}}) = y_t, \mathcal{G}(x^{\mathcal{A}}) = y_t) \quad (22)$$

$$\leq \Pr(\ell_{\mathcal{F}}(x, y_t) > \ell_{\mathcal{F}}(x, y), \ell_{\mathcal{F}}(x^{\mathcal{A}}, y) > \ell_{\mathcal{F}}(x^{\mathcal{A}}, y_t), \ell_{\mathcal{G}}(x, y_t) > \ell_{\mathcal{G}}(x, y), \ell_{\mathcal{G}}(x^{\mathcal{A}}, y) > \ell_{\mathcal{G}}(x^{\mathcal{A}}, y_t)) \quad (22)$$

$$\leq \Pr(\delta \cdot \nabla_x \ell_{\mathcal{F}}(x, y) \geq c'_{\mathcal{F}}, \delta \cdot \nabla_x \ell_{\mathcal{G}}(x, y) \geq c'_{\mathcal{G}}) \quad (23)$$

$$\leq \Pr\left(\left(c'_{\mathcal{F}} \leq \epsilon \sqrt{(1 + \bar{\mathcal{S}}(\ell_{\mathcal{F}}, \ell_{\mathcal{G}}))/2} \|\nabla_x \ell_{\mathcal{F}}(x, y)\|_2\right) \cup \left(c'_{\mathcal{G}} \leq \epsilon \sqrt{(1 + \bar{\mathcal{S}}(\ell_{\mathcal{F}}, \ell_{\mathcal{G}}))/2} \|\nabla_x \ell_{\mathcal{G}}(x, y)\|_2\right)\right) \quad (24)$$

$$\leq \Pr\left(c'_{\mathcal{F}} \leq \epsilon \sqrt{(1 + \bar{\mathcal{S}}(\ell_{\mathcal{F}}, \ell_{\mathcal{G}}))/2} \|\nabla_x \ell_{\mathcal{F}}(x, y)\|_2\right) + \Pr\left(c'_{\mathcal{G}} \leq \epsilon \sqrt{(1 + \bar{\mathcal{S}}(\ell_{\mathcal{F}}, \ell_{\mathcal{G}}))/2} \|\nabla_x \ell_{\mathcal{G}}(x, y)\|_2\right), \quad (25)$$

where Eq. 22 comes from Eqs. 16 to 19, Eq. 23 comes from Eq. 20 and Eq. 21. The Eq. 24 is a result of Lemma 8: either

$$\delta \cdot \frac{\nabla_x \ell_{\mathcal{F}}(x, y)}{\|\nabla_x \ell_{\mathcal{F}}(x, y)\|_2} \leq \|\delta\|_2 \sqrt{(1 + \bar{\mathcal{S}}(\ell_{\mathcal{F}}, \ell_{\mathcal{G}}))/2}$$

or

$$\delta \cdot \frac{\nabla_x \ell_{\mathcal{G}}(x, y)}{\|\nabla_x \ell_{\mathcal{G}}(x, y)\|} \leq \|\delta\|_2 \sqrt{(1 + \bar{\mathcal{S}}(\ell_{\mathcal{F}}, \ell_{\mathcal{G}}))/2}.$$

We observe that by  $\beta$ -smoothness condition of the loss function,

$$\begin{aligned} c'_{\mathcal{F}} &= \ell_{\mathcal{F}}(x^A, y_t) - \ell_{\mathcal{F}}(x, y) - \frac{\beta}{2} \|\delta\|_2^2 \\ &\geq \ell_{\mathcal{F}}(x, y_t) + \delta \cdot \nabla_x \ell_{\mathcal{F}}(x, y_t) - \frac{\beta}{2} \|\delta\|_2^2 - \ell_{\mathcal{F}}(x, y) - \frac{\beta}{2} \|\delta\|_2^2. \end{aligned}$$

Thus,

$$\begin{aligned} &\Pr \left( c'_{\mathcal{F}} \leq \epsilon \sqrt{(1 + \bar{\mathcal{S}}(\ell_{\mathcal{F}}, \ell_{\mathcal{G}}))/2} \|\nabla_x \ell_{\mathcal{F}}(x, y)\|_2 \right) \\ &\leq \Pr \left( \ell_{\mathcal{F}}(x, y_t) - \ell_{\mathcal{F}}(x, y) \leq \epsilon B (1 + \sqrt{(1 + \bar{\mathcal{S}}(\ell_{\mathcal{F}}, \ell_{\mathcal{G}}))/2}) + \beta \epsilon^2 \right) \\ &\leq \Pr \left( \ell_{\mathcal{F}}(x, y) \geq \ell_{\mathcal{F}}(x, y_t) - \epsilon B (1 + \sqrt{(1 + \bar{\mathcal{S}}(\ell_{\mathcal{F}}, \ell_{\mathcal{G}}))/2}) - \beta \epsilon^2 \right) \\ &\leq \frac{\xi_{\mathcal{F}}}{\min_{x \in \mathcal{X}} \ell_{\mathcal{F}}(x, y_t) - \epsilon B (1 + \sqrt{(1 + \bar{\mathcal{S}}(\ell_{\mathcal{F}}, \ell_{\mathcal{G}}))/2}) - \beta \epsilon^2}. \end{aligned} \tag{26}$$

Similarly for  $\mathcal{G}$ ,

$$\begin{aligned} &\Pr \left( c'_{\mathcal{G}} \leq \epsilon \sqrt{(1 + \bar{\mathcal{S}}(\ell_{\mathcal{F}}, \ell_{\mathcal{G}}))/2} \|\nabla_x \ell_{\mathcal{G}}(x, y)\|_2 \right) \\ &\leq \frac{\xi_{\mathcal{G}}}{\min_{x \in \mathcal{X}} \ell_{\mathcal{G}}(x, y_t) - \epsilon B (1 + \sqrt{(1 + \bar{\mathcal{S}}(\ell_{\mathcal{F}}, \ell_{\mathcal{G}}))/2}) - \beta \epsilon^2}. \end{aligned} \tag{27}$$

We conclude the proof by combining the above two equations into Eq. 25.  $\square$

**Theorem** (Upper Bound on Untargeted Attack Transferability). *Assume both model  $\mathcal{F}$  and  $\mathcal{G}$  are  $\beta$ -smooth with gradient magnitude bounded by  $B$ , i.e.,  $\|\nabla_x \ell_{\mathcal{F}}(x, y)\| \leq B$  and  $\|\nabla_x \ell_{\mathcal{G}}(x, y)\| \leq B$  for any  $x \in \mathcal{X}, y \in \mathcal{Y}$ . Let  $\mathcal{A}_U$  be an  $(\alpha, \mathcal{F})$ -effective untargeted attack with perturbation ball  $\|\delta\|_2 \leq \epsilon$ . The transferability can be upper bounded by*

$$\Pr(T_r(\mathcal{F}, \mathcal{G}, x) = 1) \leq \frac{\xi_{\mathcal{F}} + \xi_{\mathcal{G}}}{\ell_{\min} - \epsilon B \left( 1 + \sqrt{\frac{1 + \bar{\mathcal{S}}(\ell_{\mathcal{F}}, \ell_{\mathcal{G}})}{2}} \right) - \beta \epsilon^2},$$

where

$$\ell_{\min} = \min_{\substack{x \in \mathcal{X}, y' \in \mathcal{Y}: \\ (x, y) \in \text{supp}(\mathcal{D}), y' \neq y}} (\ell_{\mathcal{F}}(x, y'), \ell_{\mathcal{G}}(x, y')).$$

Here  $\xi_{\mathcal{F}}$  and  $\xi_{\mathcal{G}}$  are the empirical risks of models  $\mathcal{F}$  and  $\mathcal{G}$  respectively, defined relative to a differentiable loss. The  $\text{supp}(\mathcal{D})$  is the support of benign data distribution, i.e.,  $x$  is the benign data and  $y$  is its associated true label.

*Proof.* The proof follows the proof for the targeted attack case, but instead of  $\min_{x \in \mathcal{X}} \ell_{\mathcal{F}/\mathcal{G}}(x, y_t)$  we use

$$\min_{x \in \mathcal{X}, y' \in \mathcal{Y}: (x, y) \in \text{supp}(\mathcal{D}), y' \neq y} \ell_{\mathcal{F}/\mathcal{G}}(x, y')$$

in Eq. 26 and Eq. 27 and henceforth.  $\square$

Table 5: Robust accuracy (%) of different approaches against **blackbox transfer attack** with different perturbation scales  $\epsilon$  on MNIST dataset.

$\epsilon$	clean	0.10	0.15	0.20	0.25	0.30	0.35	0.40
Vanilla	99.5	1.8	0.1	0.0	0.0	0.0	0.0	0.0
ADP	99.4	25.5	13.8	7.0	2.1	0.3	0.1	0.0
GAL	98.7	96.8	77.0	29.1	12.8	4.6	1.9	0.6
DVERGE	98.7	<b>97.6</b>	<b>97.4</b>	<b>96.9</b>	96.2	94.2	78.3	20.2
TRS	98.6	97.2	96.7	96.5	<b>96.3</b>	<b>95.5</b>	<b>93.1</b>	<b>86.4</b>

Table 6: Robust accuracy (%) of different approaches against **blackbox transfer attack** with different perturbation scales  $\epsilon$  on CIFAR-10 dataset.

$\epsilon$	clean	0.01	0.02	0.03	0.04	0.05	0.06	0.07
Vanilla	94.1	10.0	0.1	0.0	0.0	0.0	0.0	0.0
ADP	91.6	20.7	0.5	0.0	0.0	0.0	0.0	0.0
GAL	88.3	74.6	58.9	39.1	22.0	11.3	5.2	2.1
DVERGE	91.9	<b>83.3</b>	69.0	49.8	28.2	14.4	4.0	0.8
TRS	86.7	78.3	<b>69.3</b>	<b>55.3</b>	<b>43.2</b>	<b>30.1</b>	<b>22.4</b>	<b>13.1</b>

## D Training Details

We adapt ResNet-20 [23] as the base model architecture and Adam optimizer [26] in all of our experiments.

**Baseline Training.** For ADP and GAL, we follow the exact training configuration mentioned in their paper in both MNIST and CIFAR-10 experiments. For DVERGE, we set the same feature distillation  $\epsilon = 0.07$  with step size as 0.007 for CIFAR as they mentioned in their paper but set  $\epsilon = 0.5$  with step size as 0.05 for MNIST since they didn't conduct any MNIST experiments in their paper.

**TRS Training.** For MNIST, we set the initial learning rate  $\alpha = 0.001$  and train our TRS ensemble for 120 epochs by decaying the learning rate by 0.1 at 40-th and 80-th epochs. For CIFAR-10 and CIFAR-100 we set the initial learning rate  $\alpha = 0.001$  and train our TRS ensemble for 200 epochs by decaying the learning rate by 0.1 at 100-th and 150-th epochs.

## E Numerical results of Blackbox robustness evaluation

Table 5 and 6 show the detailed robust accuracy number of different ensembles against blackbox transfer attack with different perturbation scale  $\epsilon$ , which corresponds to the Figure 3. As we can see, TRS ensemble shows its competitive robustness to DVERGE on small  $\epsilon$  setting but much better stability of robustness on large  $\epsilon$  setting even with the lowest benign accuracy on clean data.

## F TRS ensemble under various hyper-parameter settings

We explore various hyper-parameter settings on  $\lambda_a, \lambda_b, \delta_M$  for TRS training and obtain series of ensembles with stable robustness. Table 7 shows the results containing the whitebox robustness of TRS ensembles trained with  $\lambda_a \in \{100, 500\}, \lambda_b \in \{2.5, 10\}, \delta_M \in \{0.3, 0.4\}$  combination configurations. As we can see, different configurations will lead to similar ensemble robustness and almost all of them could still beat other baseline works. This indicates that we don't need to tune the TRS training hyper-parameters too much when we utilize

Table 7: Robust accuracy (%) of TRS ensemble trained with different hyper-parameter settings against various whitebox attacks on MNIST dataset.

$\lambda_a$		100				500			
$\lambda_b$		2.5		10		2.5		10	
$\delta_M$		0.3	0.4	0.3	0.4	0.3	0.4	0.3	0.4
FGSM	$\epsilon = 0.1$	<b>95.6</b>	94.6	90.6	94.8	<b>95.6</b>	93.0	95.2	93.6
	$\epsilon = 0.2$	91.7	83.4	89.7	87.3	<b>92.0</b>	84.0	88.0	85.0
BIM (50)	$\epsilon = 0.1$	<b>93.3</b>	82.9	75.7	92.5	88.2	83.9	92.6	90.9
	$\epsilon = 0.15$	<b>85.7</b>	69.7	61.3	84.1	73.1	61.3	82.2	83.3
PGD (50)	$\epsilon = 0.1$	<b>93.0</b>	79.1	74.3	92.2	86.3	83.3	91.7	90.6
	$\epsilon = 0.15$	<b>85.1</b>	62.6	57.4	82.6	69.9	58.2	80.0	82.9
MIM (50)	$\epsilon = 0.1$	<b>92.9</b>	81.6	75.1	92.0	87.7	83.5	91.7	91.2
	$\epsilon = 0.15$	<b>85.1</b>	68.2	60.2	83.7	74.0	62.4	82.4	83.4
CW	$c = 0.1$	98.1	96.6	96.4	97.5	<b>98.4</b>	97.2	98.1	97.8
	$c = 1.0$	92.6	92.6	89.1	<b>95.9</b>	86.1	77.4	88.2	95.1
EAD	$c = 1.0$	23.3	14.3	9.2	<b>24.1</b>	22.5	2.6	3.4	23.9
	$c = 5.0$	1.4	0.9	0.1	<b>2.3</b>	0.0	0.0	0.2	1.7
APGD-DLR	$\epsilon = 0.1$	<b>92.1</b>	78.5	72.8	91.5	85.9	82.8	91.1	90.2
	$\epsilon = 0.15$	<b>83.4</b>	62.1	57.0	82.3	69.6	57.9	79.8	82.4
APGD-CE	$\epsilon = 0.1$	<b>91.7</b>	78.1	72.1	91.2	85.2	82.5	90.8	89.7
	$\epsilon = 0.15$	<b>82.8</b>	61.3	56.5	81.9	69.3	57.6	79.4	81.7

the TRS regularizer into new classification tasks.

## G Robustness on CIFAR-100 dataset

Besides MNIST and CIFAR-10 datasets, we also evaluate our proposed TRS ensemble on the CIFAR-100 dataset. The base model structure and training parameters configuration remain the same as in CIFAR-10 experiments. The whitebox robustness evaluation results are shown in Table 8. From the results, we can see that the robustness of TRS model is better than other works against all attacks except FGSM, which is similar with our observations in CIFAR-10. This shows that our TRS algorithm still achieves a good performance on classification tasks with large number of classes.

Table 8: Robust accuracy (%) of different approaches against various whitebox attacks on CIFAR-100 dataset.

CIFAR-100	para.	ADP	GAL	DVERGE	GST-TRS
FGSM	$\epsilon = 0.02$	11.5	28.7	<b>29.7</b>	19.3
	$\epsilon = 0.04$	6.4	2.7	<b>25.4</b>	9.5
BIM (50)	$\epsilon = 0.01$	0.5	7.6	12.1	<b>22.9</b>
	$\epsilon = 0.02$	0.0	1.5	2.9	<b>5.4</b>
PGD (50)	$\epsilon = 0.01$	0.4	5.4	11.3	<b>23.0</b>
	$\epsilon = 0.02$	0.0	1.1	2.0	<b>5.3</b>
MIM (50)	$\epsilon = 0.01$	0.5	5.7	13.1	<b>23.4</b>
	$\epsilon = 0.02$	0.0	0.5	2.6	<b>6.2</b>
CW	$c = 0.01$	11.3	32.0	44.8	<b>45.7</b>
	$c = 0.1$	0.5	10.7	20.3	<b>26.9</b>
EAD	$c = 1.0$	0.0	0.0	1.0	<b>5.7</b>
	$c = 5.0$	0.0	0.0	0.0	<b>0.3</b>
APGD-LR	$\epsilon = 0.01$	0.2	4.3	11.8	<b>22.2</b>
	$\epsilon = 0.02$	0.0	0.6	2.1	<b>5.3</b>
APGD-CE	$\epsilon = 0.01$	0.2	4.2	11.3	<b>20.7</b>
	$\epsilon = 0.02$	0.0	0.4	1.7	<b>4.8</b>